Redesigning Liver Allocation Regions through Optimization

by

Timothy Scully

B.A. Mathematics, Tufts University (2011)

Submitted to the Sloan School of Management
in partial fulfillment of the requirements for the degree of

Master of Science in Operations Research

at the

MASSACHUSETTS INSTITUTE OF TECHNOLOGY

June 2017

Signature redacted

Author .....
Sloan School of Management
May 19, 2017

Signature redacted

Certified by... .....
Jónas Oddur Jónasson
Assistant Professor of Operations Management
Thesis Supervisor

Signature redacted

Certified by..... .....
Nikolaos Trichakis
Zenon Zannetos (1955) Career Development Professor and Assistant Professor of Operations Management
Thesis Supervisor

Signature redacted

Accepted by ....
Dimitris Bertsimas
Boeing Professor of Operations Research,
Co-Director, Operations Research Center

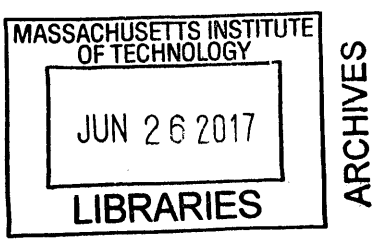

Redesigning Liver Allocation Regions through Optimization

by

Timothy Scully

Submitted to the Sloan School of Management
on May 19, 2017, in partial fulfillment of the
requirements for the degree of
Master of Science in Operations Research

Abstract

End-stage liver disease is one of the leading causes of death in the United States, and the only viable treatment is liver transplantation. Since the quality of a donor liver decreases with transportation time, United States organ policy prioritizes transplants within geographic regions. However, the boundaries of these regions were defined mostly by informal relationships between transplant centers many decades ago, which has created local imbalances in supply and demand. As a result, candidates on the waiting list for donor livers face drastically different odds of receiving a transplant. Policy makers have noticed this geographic inequity and are considering proposals for alternative liver allocation approaches.

This thesis uses mathematical optimization to redesign liver allocation regions by modeling and including several key elements of the allocation process directly in the optimization formulation. Specifically, we use a fluid approximation to model the dynamics of the waitlist progression and liver allocation. The model is fit using historical data of waitlist candidates and donors. Then, we propose two optimization formulations to reduce geographic inequality. The first directly minimizes the variation in median level of illness at the time of transplant across geographical areas, which is a key metric used by policy makers in addressing geographic inequality. The second approach minimizes the liver transport distance, subject to a certain allowable level of geographic variation. We discuss how these models can flexibly incorporate additional policy constraints to create more realistic models to reduce geographic variation. The region configurations are evaluated on key metrics relating to fairness and system efficiency using a standardized, validated, simulation approach widely accepted by policymakers. Finally, we propose a region design that significantly reduces geographic inequality without any substantial impact on the system's efficiency.

Thesis Supervisor: Jónas Oddur Jónasson
Title: Assistant Professor of Operations Management

Thesis Supervisor: Nikolaos Trichakis
Title: Zenon Zannetos (1955) Career Development Professor and Assistant Professor of Operations Management

Acknowledgments

I would to thank Professors Jónas Jónasson and Nikos Trichakis for their enormous effort in shaping this research. Without your insightful comments, suggestions, and ideas, this thesis would not have been possible. Additionally, I would like to thank Dr. Parisa Vagefi and Dr. Madhukar Patel at Mass General Hospital, who provided invaluable feedback on this research. Furthermore, I want to thank the staff at the Scientific Registry of Transplant Recipients, who provided us with the data that made this project possible.

I also want to thank everybody who made the ORC such a challenging and welcoming environment. In particular, I would like to thank Dimitris Bertsimas and Patrick Jaillet, who helped me navigate academic and research opportunities.

Finally, I want to thank my fiancée, who made graduate school an experience I will always look back on with the fondest memories.

THIS PAGE INTENTIONALLY LEFT BLANK

Contents

THIS PAGE INTENTIONALLY LEFT BLANK

List of Figures

THIS PAGE INTENTIONALLY LEFT BLANK

List of Tables

THIS PAGE INTENTIONALLY LEFT BLANK

Chapter 1

Introduction

End-stage liver disease is the 12th leading cause of death in the United States, with over 40,000 deaths reported in 2015 [27]. The only treatment for end-stage liver disease is liver transplantation. In the United States, all potential candidates are required to a join a waitlist. Livers are then allocated to candidates based primarily on medical urgency and geographic distance from the donor. Since the quality of the liver deteriorates with transportation time, it is preferable to allocate the organ to nearby patients, all else equal. To prioritize nearby patients, the liver allocation system is divided into geographical regions. When a liver is recovered from a deceased donor in a region, patients residing within the region are prioritized over others. However, the formation of the region boundaries was based on informal relationships between transplant hospitals, not a concerted effort to create an efficient or fair system. Therefore, these regions contribute to drastic imbalances in supply and demand. As a result, patients often face very unequal prospects of receiving a donor-liver based on where they reside. Policy makers have noticed this geographic inequity and passed an aspirational guideline, called the Final Rule, which states that the place of listing shall not be a major determinant in liver allocation. This proclamation resulted in several adjustments to the allocation policy, but the geographic inequity persists today.

In this thesis, we use mathematical optimization to redesign the liver allocation regions to reduce geographic inequity. We incorporate several key facets of the allocation system directly into the optimization framework. Specifically, we approximate

the dynamics of the wait list and allocation system using a fluid model. Based on this framework, we present two optimization models aimed at reducing geographic variation. Simulation results indicate that the optimized regions result in far less geographic inequity without a significant decrease in system efficiency. Based on this analysis, we propose a new region design and compare it with the existing regions, as well as other proposals.

The organization of the thesis is as follows: the remainder of this chapter will describe the allocation process and discuss the problem of geographic inequity. Chapter 2 provides a review of previous research on redesigning liver regions through optimization. Chapter 3 presents a concrete redistricting strategy that reduces geographic variation, while maintaining the efficiency of the system. Chapter 4 introduces a fluid model approximation to the liver waiting list and allocation system. Chapter 5 describes the estimation of the parameters used in the optimization, such as the disease progression matrix. Chapter 6 proposes an optimization formulation that incorporates the fluid model to directly minimize a key metric of geographic variation. Chapter 7 proposes an optimization formulation that minimizes the total transport time of the organs within some allowable regional variation. Chapter 8 discusses the limitations of our approach and potential extensions, and chapter 9 provides a conclusion.

1.1 Liver Allocation System

Donor livers are a scarce resource; there are many more individuals entering the waitlist than there are donors available for transplantation. As a result of this drastically insufficient organ supply, 1,478 people died in 2015 while waiting for a liver, and another 1,510 were removed because they were too sick to undergo surgery for transplantation. Therefore, the challenge in the liver allocation system is to develop a set of guidelines that allocates the scarce resource to candidates.

Figure 1-1: Donor Service Areas

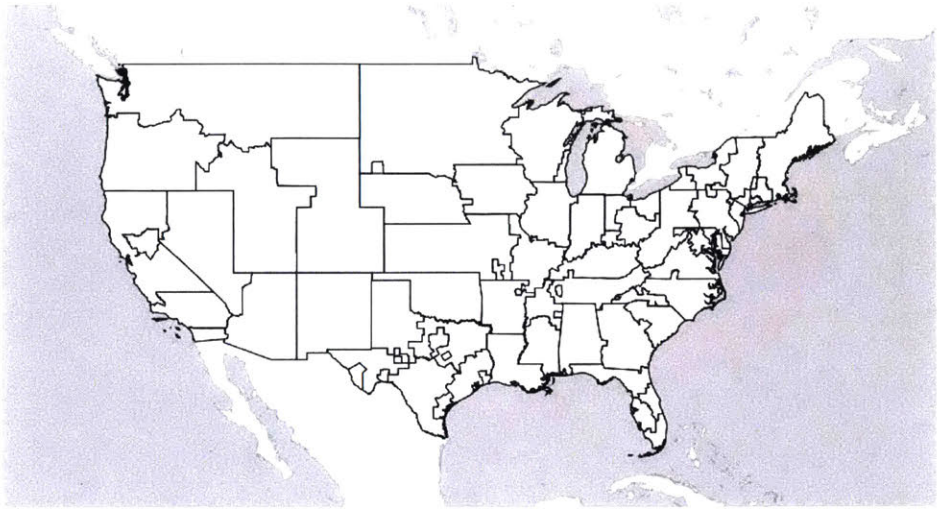

1.1.1 Organizations and Geographical Areas

In the United States, the United Network for Organ Sharing (UNOS) is the organization that administers the Organ Procurement and Transplantation Network (OPTN), which determines the allocation policy. This responsibility includes keeping detailed records for each wait list candidate, which are used in the matching process when a liver becomes available. Furthermore, UNOS is also charged with overseeing 58 local organ procurement organizations (OPOs). Each OPO is responsible for enforcing the allocation system for a fixed geographic region, including registering patients to the liver waitlist, coordinating organs from donor hospitals, matching donor organs to recipients, and arranging the transportation of the recovered organ to the matched candidate. The geographic area that each OPO presides over is called the donor service area (DSA), which can range from a metropolitan area to several states. The map of the OPOs and corresponding DSAs is shown in Figure 1-1. DSAs are further grouped into 11 larger geographic areas called regions, as shown in Figure 1-2.

1.2 Role of Geographical Areas in Allocation

Geographic areas are critical to the liver allocation process because the quality of the liver decreases with the time required to transport the liver from the donor to recipi-

Figure 1-2: Existing 11 Regions

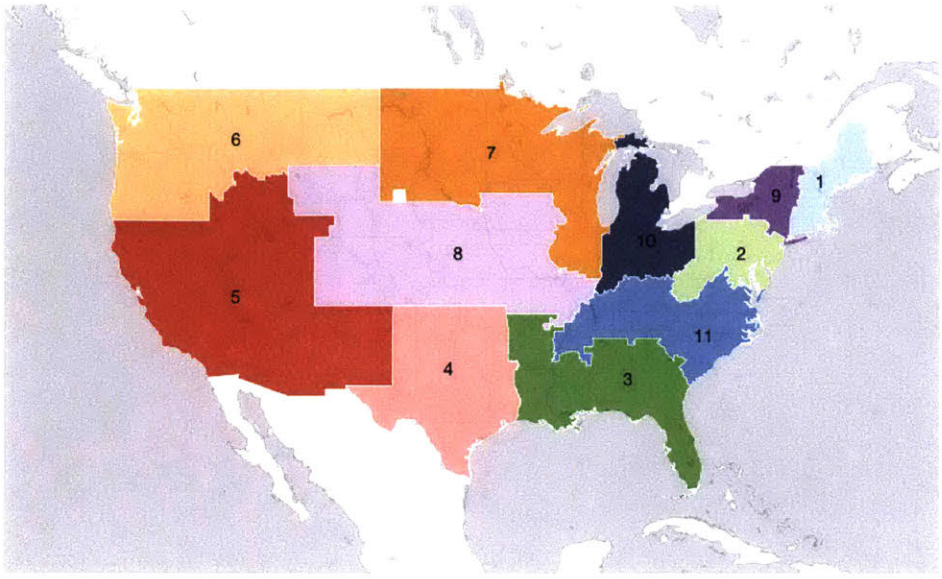

ent. Specifically, the cold ischemia time (CIT), the amount of time that a liver needs to be chilled between recovery from the donor and transplantation, negatively effects the outcomes of the liver transplant [23]. Therefore, all else equal, transplantations that require a shorter transport time are preferable, since they result in better post-transplant outcomes. Hence, geographic areas (DSA and regions) are intended to prioritize transplants to candidates that are geographically near the deceased donor.

However, livers also need to be prioritized to the patients that most need them. For instance, it is easy to imagine a liver recovered in California, but the most urgent candidate resides in Massachusetts. While always providing the liver to the most medically urgent patient may be fair in some sense, it also reduces the efficiency by allowing large liver transport times. Therefore, the liver allocation system is designed to prioritize the most sick patients, while preserving the overall efficiency of the system by prioritizing patients within geographical areas.

1.2.1 Allocation of Livers

In general, the allocation follows a three tier system. First, the liver is offered within the local DSA. If the liver is declined or no such candidate exists, it is then offered to the region level. Finally, if there is no match at the region level, it is then offered to

the national level. Within this geographical hierarchy, patients are prioritized based on medical urgency and blood compatibility.

In order to quantify medical urgency, UNOS has established a metric called a MELD score, which reflects the estimated 3-month waiting list mortality [10]. MELD scores range from 6 (least sick) to 40 (most sick). Therefore, livers are allocated to patients based on descending MELD score, all else equal. MELD scores have shown to be an accurate metric to determine disease severity [16]. However, for a subset of candidates with certain disease types, a MELD score does not accurately reflect their mortality risk. Therefore, exception points were introduced to handle these cases. Together with exception points, MELD scores allow candidates to be ranked on their relative urgency for a liver transplants. Furthermore, patients with fulfillment liver failure and have a life expectancy of less than 7 days are designated as Status 1, which is prioritized over all MELD scores. In addition to medical urgency, blood compatibility also factors into the allocation process. Because donor livers and transplant candidates need to be medically compatible to allow for a successful transplant, patients with a blood type compatible with the donor liver are prioritized over those with incompatible or less compatible blood types. [21] provides a thorough summary of the effect of blood type compatibility on liver transplantation. Furthermore, age of donor, age of candidate, and the amount of time the candidate has been waiting also factor into the allocation process.

Therefore, the allocation policy combines the geographical hierarchy with priority given to compatible individuals with higher medical urgency. The allocation rules for adult donors are shown in Table A.2. The allocation rules vary slightly by the categorization of the donor. For a full set of rules, refer to OPTN [19]. However, the allocation for adult donors constitute the vast majority of all transplants and reflect the key elements of the allocation process.

Since 2010, there have been changes to the liver allocation process, described in section 1.3.1. However, the prioritization of candidates in the local DSA and larger region remains. Therefore, the boundaries of these geographical regions have a profound effect on both the fairness and efficiency on the allocation. While the

boundaries of the DSAs are fairly rigid due to operational and administrative constraints, the boundaries of the regions can be changed more easily. Therefore, this thesis aims to find new region boundaries that not only reduce geographic inequity, but also minimize the travel-time of livers and thereby improve the efficiency of the system.

1.3 Problem of Geographic Inequity

Despite efforts in the past 10 years to reduce variation in access to livers, severe geographic disparities remain. The existing regions were created based on regional relationships between transplant centers several decades ago [13]. As a result, some regions now have drastically different supply and demand for livers than others. The worsening donor liver shortage has exacerbated the regional disparities. This fundamental disparity is reflected in many facets of the allocation system. For instance, a candidate with a MELD of 38 might face an 18% chance of transplant within 90 days in one DSA, versus 86% in another [20]. Similarly, the death rates for OPOs can vary by as much as a factor of 4 [18]. The geographic disparity can be seen more generally in the drastic difference between the actual supply in each DSA and the number of transplants that would occur without any geographic constraints on the allocation process. The map, shown in Figure 1-3, reveals that some regions have demand over 3 times greater than the supply of livers. However, the geographic disparity is perhaps best demonstrated by the variation in median MELD across geographic areas. In the absence of geographic disparity, the MELD scores at which patients receive transplants would be consistent across regions, since allocation is largely dictated by MELD within a given region. However, as recently as 2013, the average transplant MELD varied by as much as 7 points across regions.

1.3.1 Policies Enacted by OPTN

Over the past several years, OPTN has revised several aspects of the liver allocation process. This section provides a chronological description of key developments, in

Figure 1-3: Percent Difference in Ideal Demand and Actual Supply, by DSA

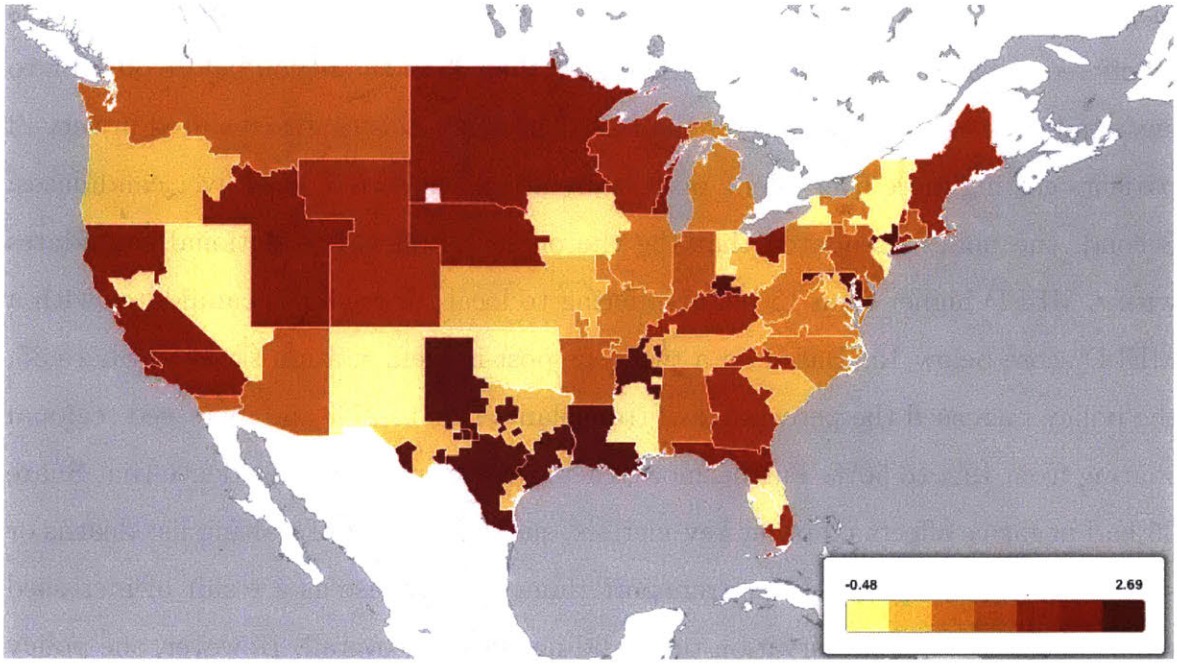

order to provide context to our efforts to reduce geographic variation.

Because of the geographic inequality in liver transplantation, the US Department of Health and Human Services enacted an aspirational guideline called the Final Rule, which stated that place of residence or listing shall not be a major determinant of organ allocation [8]. This declaration prompted the subsequent policy changes.

In 2005, OPTN implemented a new allocation policy, called the Regional Share 15 rule. This policy offered organs to patients with a MELD greater than 15 on a local and region scale before offering to a local candidate with MELD below 15. This change was prompted by medical evidence that suggested there was a positive average survival benefit for candidates with a MELD score above 15, but a negative survival benefit for those below 15. Analysis showed that the variations in median MELD at transplant actually increased among DSAs [9]. The Liver Committee distributed a request for feedback on the current liver allocation from the transplant community and academia in December of 2009 and then hosted a public forum in April of 2010 to explore various approaches to reduce geographic disparity [15].

As a result of the request for information and public forum, the Regional Share 35

Rule was approved in June 2012 and implemented in 2013 [15]. This policy made two major changes to the existing allocation rules. First, the policy mandated that organs be offered to candidates with a MELD higher than 35 in the region before offering to any candidate with a MELD lower than 35. Therefore, this change resulted in very ill patients getting more liver offers, potentially at the expense of local liver candidates. Second, the policy mandated that the the organ be offered to national candidates with a MELD higher than 15 before offering to local (or regional) candidates with a MELD score below 15. Based on a two year post-implementation study of Share 35, the policy increased the percentage of transplants 19% to 27% and increased regional sharing from 19% to 50%. Furthermore, there was no substantial evidence that Share 35 had negative effects on other key metrics, such as number of waiting list deaths or survival after transplant. Liver transport times did increase as a result of increased regional sharing, but preservation times did not increase overall. However, the policy did not do much to remove the geographic disparity in severity of disease among the regions [15].

One conclusion from this exercise was that broader sharing has been constrained by the current geographic borders. So, in order to solve the geographic disparity, it is necessary redefine the regions. In November 2012, OPTN/UNOS Board officially declared that the existing geographic disparity was unacceptably high. As a result, OPTN requested that the liver committee investigate alternatives to DSA boundaries and consider optimization as an method.

In June 2014, OPTN released a concept paper highlighting the potential of redistricting as a method to minimize geographic disparity in liver allocation [18]. The concept paper provided strict guidelines that any redistricting proposal would have to meet. Specifically, a) the number of districts should be at least 4 and no more than 8; b) the minimum number of transplant centers per district is 6; c) the maximum median travel time between DSAs in the same district is 3 hours; d) the number of waitlist deaths under redistricting must not be statistically significantly higher than the current system;) the districts should be contiguous. As a result of feedback from the redistricting concept paper, OPTN proposed an 8 region redistricting proposal

Figure 1-4: OPTN Proposed 8 Regions [19]

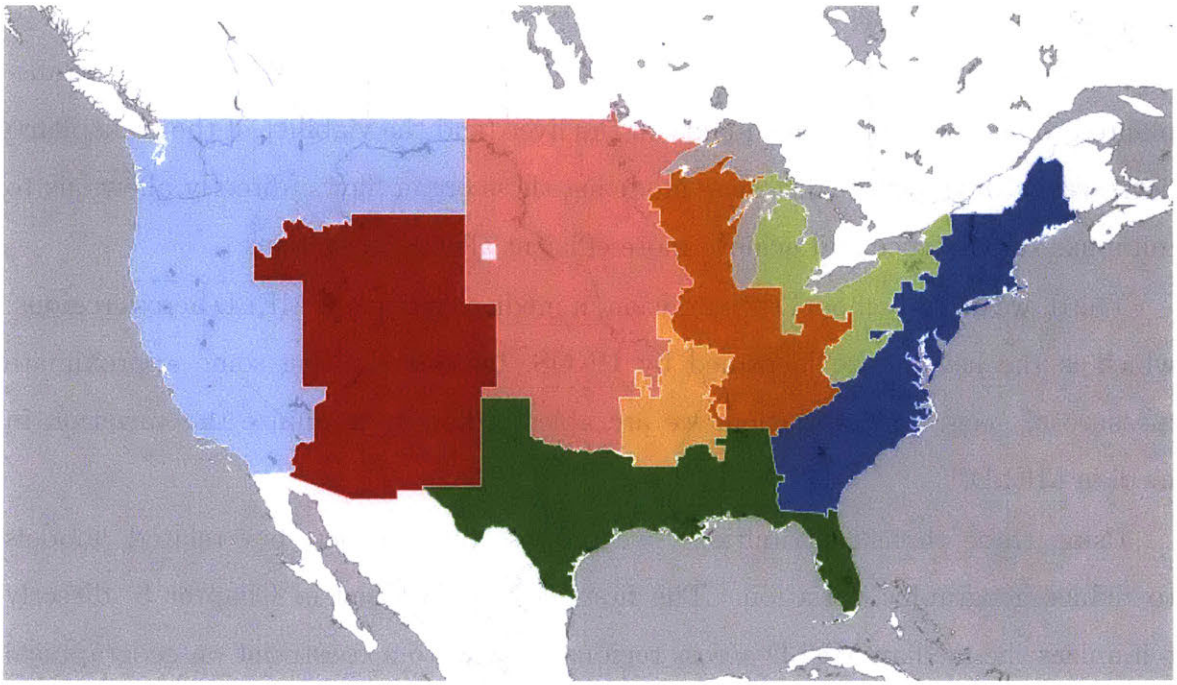

based on mathematical optimization and opened up the proposal for public comment [19]. The proposed regions are shown in Figure 1-4. The proposal also modified the ranking of candidates for a given liver. The full allocation rule is shown in A.3. The new allocation uses a regional sharing cutoff of 29 and a national sharing cutoff of 15. This proposal, as well the underlying optimization formulation developed by Gentry et al., will be a key baseline for our research. In Chapters 3, 6 and 7 we compare the results of our models with this proposal.

1.4 Thesis Contributions

We propose three key contributions to region design optimization methods. First, we propose a fluid model approximation to the liver allocation system. This approach, described in Chapter 4, approximates the steady state number of wait listed individuals and the number of transplants at each MELD state. Using an estimated MELD-state transition matrix, the approximation captures the key aspects of the waiting list and allocation system. This approximation is directly embedded in the

optimization models to reduce geographic variation.

Second, we use this approximation of the waiting list and allocation process to model the number of livers that are recovered from one geographic area and transplanted to another. Since the quality of the liver (and the viability of the transplant) decreases with transport distance, modeling these organ 'flows' directly allows us to minimize the distance and achieve more efficient allocation systems.

Third, we directly model the variation in median transplant MELD across regions, which is the key metric identified by UNOS. Instead of using some approximate measure of geographic variation, we are able to directly minimize the variation in median MELD.

Using these three contributions, we propose two distinct, but related, models to reduce geographic variation. The first model, discussed in Chapter 6, directly minimizes the median MELD across regions, subject to a constraint on geographical region size. The second model, discussed in Chapter 7, minimizes the total liver travel time in the allocation system, subject to some degree of geographic variation.

For each year between 2010 and 2015, we estimate the input parameters, and then formulate and solve the optimization problem. The parameters are estimated from historical liver waitlist and transplant obtained from the Scientific Registry of Transplant Recipients The data contains historical records of candidates on the waitlist, including registration, status updates, removals, transplants, and death in the United States. Furthermore, the data also contains detailed information about the donors, the transplant process, and post-transplant records. The input parameters, described in 5, are estimated from the SRTR data. Then, we test the performance of the optimized regions by simulating, as described below.

1.5 Proposal Evaluation Methodology

The optimized regions are evaluated using a validated simulation approach called Liver Simulated Allocation Model (LSAM). LSAM captures the key events in the allocation process, including patient arrivals, liver arrivals, liver offers to candidates,

candidates' acceptance decision, MELD transitions, removal from the waitlist, and post-transplant outcomes. Using the simulated results, we are able to analyze the effect of a proposed policy on key metrics, such as geographic variation in MELD at transplant, distance traveled, number of waitlist deaths, and median wait time before receiving a liver. Furthermore, the simulation output allows us to analyze how a proposed policy affects certain subpopulations based on age, income, or race. LSAM is a widely used by policymakers to determine the effect of an allocation policy change. Therefore, the results are easily interpretable and comparable against other models and policy analysis.

Since this research is focused on designing optimal regions and not modifying the allocation rule, we treat the allocation rules as fixed. Specifically, we use the current allocation scheme (Share 35) as shown in Table A.2. Although the allocation rule will affect the overall system, we fix the allocation rule and test the effect of region design. We simulate the allocation system from January 1, 2010 to December 31st, 2010.

THIS PAGE INTENTIONALLY LEFT BLANK

Chapter 2

Literature Review

Many researchers have applied mathematical modeling and optimization to solve problems related to organ allocation. Previous work on liver allocation can be broadly categorized into three groups: 1) determining optimal decisions in liver allocation; 2) evaluating of allocation policies; and 3) and redesigning liver regions through optimization. While the first two areas of research are related to this thesis, the third section is the most directly relevant. Therefore, this section will describe the previous work on mathematical optimization approaches to redesign the liver allocation regions. We refer to [4] for a more complete literature review on the first two areas of research.

Stahl et al. first applied optimization methods to liver allocation design in 2005, when they developed a methodological framework to determine region configurations that maximize transplant allocation efficiency and geographic equality [24]. This research used an integer programming formulation to maximize a weighted combination of two objectives - the number of intraregional transplants and the lowest intraregional transplant rate across all regions. The framework incorporated estimated function between travel time and liver viability. Specifically, they made the simplifying assumption that the probability of rejecting a liver was solely dependent on CIT. Furthermore, the number of OPOs in any region was limited to 9 due to computational constraints. The authors conclude that the optimized regions resulted in up to 17 additional transplants, thereby increasing the efficiency of the system. Fi-

nally, they highlight the tradeoff between system efficiency and geographic variation by varying the model parameter governing the tradeoff in the objective function.

Kong et al. also developed optimization formulations to redistrict the liver regions in the United States. This work aimed to maximize the efficiency of the intraregional transplants, without considering geographic variation. To do this, they defined an estimate of viability-adjusted transplants to capture the trade offs between large and small regions. Larger regions resulted in better matching but greater transport distance compared to smaller regions. Therefore, the estimate of viability-adjusted transplants captured these competing forces of region size. The model made the simplifying assumption that the transplant benefit depends only on liver transport distance. Therefore, the transplant benefit is identical for donors with different clinical and demographic characteristics, which greatly simplifies the dynamics of liver allocation described in Chapter 1. The optimization was solved with a branch and price algorithm, with a geographic decomposition using geographic covers to generate promising columns quickly in the pricing problem. Although they concluded that the quality of the solution depended on the geographic covers, they estimated that the optimized regions might result in an increase of 90 transplants per year.

Demirici et al [7] extended this framework to account for the trade-off between efficiency and geographic equity in the liver allocation process [7]. Using an exact branch-and-price approach, Demirici et al. were able to approximate the frontier of Pareto-efficient solutions with respect to the objectives of efficiency and geographic equity. Using this framework, they considered many districts that Stahl et al. excluded. Testing the framework on observed data, they concluded that there exist regions that significantly dominate the current configuration with regards to both efficiency and geographic equity, suggesting that the liver allocation process can be improved through reorganizing the existing regions. In both of these frameworks, the geographic equity metric is modeled as the maximum of the minimum in-district viability-adjusted transplant rates. Critics argue that this metric is not suitable for geographic disparity, since the transplant rates per candidate are sensitive to differences in waitlisting patterns across DSAs, which can distort the number of waitlisting

list candidates [14].

Finally, Gentry et al. proposed a framework that forgoes modeling efficiency and instead only models geographic disparity. The framework minimized the sum of absolute differences between the supply of donor livers in a region and the ideal number of livers that would be offered in each region if each liver was allocated based entirely on medical urgency. The model included constraints imposed by policy makers, including requiring the regions to be compact, contiguous, and bounded by some allowable size.

This model abstracts away from key dynamics, such as liver quality, and instead models rates of supply and demand. Therefore, this model is drastically simpler than the previous approaches discussed here and can be solved to optimality using off-the-shelf solvers in less than an hour. Despite the model's simplicity, the resulting regions are able to substantially reduce the geographic variation. Using simulation to test the regions, Gentry et al. showed that the resulting regions reduced the geographic variation by between 30-70%, depending on the number of regions use. Although Gentry et al.'s formulation minimized the number of misdirected livers, UNOS has focused on the standard deviation in the median transplant MELD score across regions as the key metric to evaluate geographic disparity. Compared to a standard deviation of 3.0 under local (DSA) allocation, the optimized 8 region with a 4 hour travel time limit resulted in a standard deviation of approximately 2. The optimized 8 regions would result in slightly higher median travel time and distance, percent flying, and cost of transporting the livers compared to local allocation. However, Gentry et al. estimated that the total cost of the new regions would be less than local allocation due to cost savings elsewhere. This model forms the foundation for the OPTN's 8 region reformulation proposal currently out for public comment. Therefore, we will often treat this model as a baseline to compare our approach.

The previous approaches either aims to improve system efficiency [17], geographic fairness [14], or both [7, 24]. Furthermore, previous work varies substantially in how they choose to model the allocation process. Simple models, such as [14], only consider rates of supply and demand, while others [7, 24] directly model aspects of

the allocation system in the optimization.

This thesis aims to reduce geographic variation while minimally impacting efficiency. To do so, we propose an approximation of the dynamics of the waitlist and the allocation process. Therefore, unlike all previous work, we are directly including a model of the dynamics of the allocation process directly in the model. Furthermore, previous research uses rough estimates of geographic fairness. For instance, [24] used the lowest intraregional transplant rate across all OPOs as a measure of geographic equity. Similarly, [14] used the sum of absolute difference in rates of supply and demand. Although both metrics reflect overall geographic variation, they do not necessarily reflect the metrics used by policy makers. Therefore, we use a more precise measure of geographic variation, as determined by policymakers. Specifically, we model geographic inequity as the variation in the median transplant MELD across regions.

Lastly, unlike most other approaches ([24, 17, 7]), our model reflects the policy guidelines established by OPTN. We follow the precedent of Gentry et al. and use validated simulation approach to evaluate region design. Therefore, our results and insights can be more directly applied by policy makers and potentially affect the region design.

Chapter 3

A Redistricting Proposal

In this chapter, we present a new region design for liver allocation based on the subsequent analysis in Chapters 4 through 8. The region configuration was optimized to minimize geographic inequity without impacting efficiency. The proposed regions are shown in Figure 3-1[1]. Using simulation results, we compare this proposed region configuration to both the current regional configuration and the 2016 OPTN proposal. We compare the proposals based on geographical variation, liver transport distance, number of transplants, and the number of deaths. We conclude that our proposal results in a 10% reduction in standard deviation of median transplant MELD, while only increasing median transport time by 1%. Full results are shown in Table 3.1.

3.1 Geographic Variation

In our proposal, the median MELD ranges from 24 to 29 across the regions. The standard deviation of the regional median MELD would be 1.5. Figure 3-2a shows the regional variation in median MELD. The west coast exhibits higher median MELD at transplant due to high demand for livers relative to supply. However, the remainder of the country exhibits relatively uniform median transplant MELD, ranging between 24 to 26.

Figure 3-2b shows the geographic variation under the current 11 region configu-

[1]DSA in Hawaii belongs to region 2; DSA in Puerto Rico belongs to region 3

ration, which has a standard deviation of regional median transplant MELD of 2.95 - almost twice as large as our proposal. Similarly, Figure 3-2c shows the simulated geographic variation under the 2016 OPTN redistricting proposal. While the proposal results in lower variation than the existing regions, there is still considerable regional variation. The range in median transplant MELD is 23 to 29, and the standard deviation is 1.77. Our proposal results in significantly lower geographic variation than both the current configuration and the 2016 proposal. Furthermore, in all three configurations, the west coast exhibits the highest median MELD. This suggests there is a certain level of unavoidable variation, since there are not sufficient low demand regions nearby to balance the high demand of the west coast.

Figures 3-3a, 3-3b, and 3-3c show a box-plot graph of geographic variation for our region proposal, the current system, and the 2016 OPTN proposal respectively. In addition to reducing variation in median MELD across the regions, our proposal also results in less variation within the regions, compared to the current system. Our proposal results in similar within-region variation compared to the 2016 proposal.

Figure 3-1: Proposed Regions

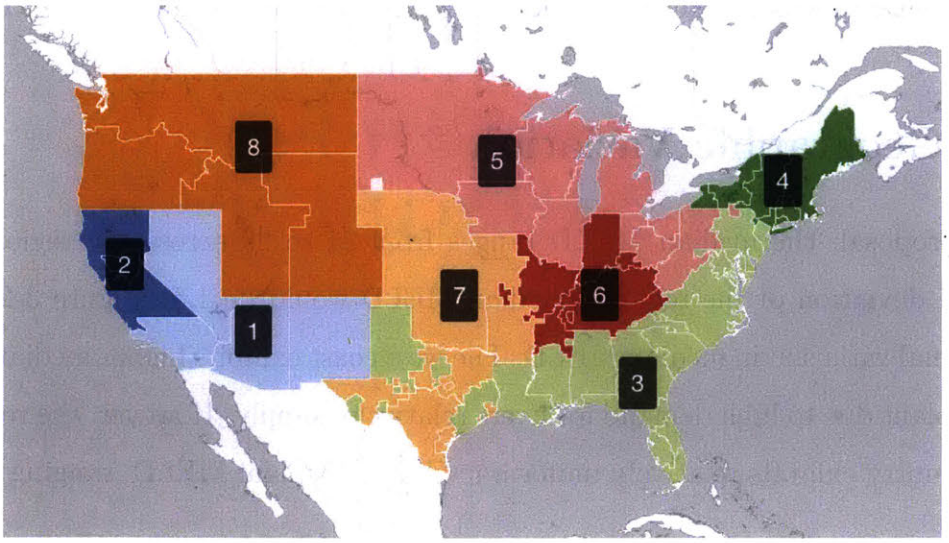

Figure 3-2: Median MELD by Region

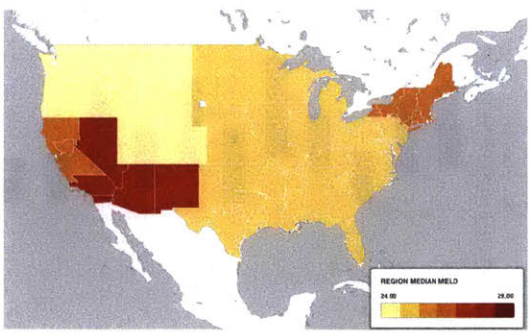

(a) Our Proposal

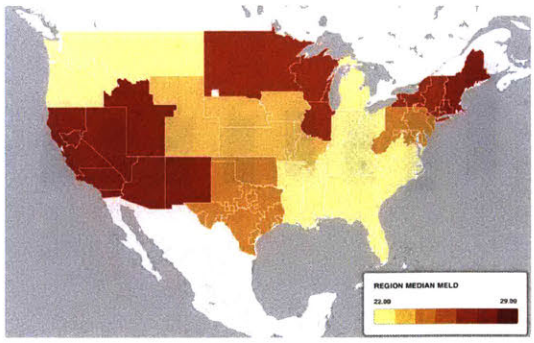

(b) Current 11 Regions

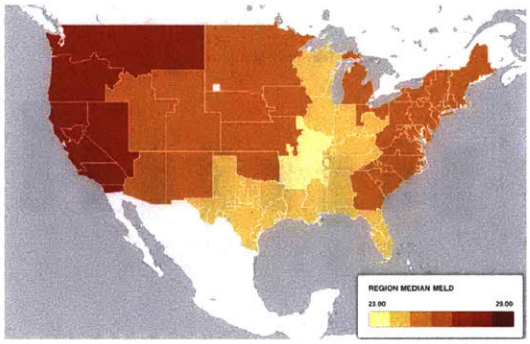

(c) 2016 OPTN Proposal

3.2 Key Metrics

However, geographic variation is not the only consideration when evaluating an allocation process. Table 3.1 shows additional key allocation metrics based on the simulation results. Compared to the 2016 proposal, the median travel time slightly increases by 1.2% under our proposal. Similarly, median distance increases by 2.3%. However, the percent of organs flown does not increase at 53%.

Furthermore, our proposal results in fewer waitlist deaths than the 2016 proposal, but roughly the same number of total deaths. Under all three region designs, the median post-graft life years is 5. In addition, our proposal results in a smaller number of national transplants, which reflects positively on the efficiency of the system.

Based on these simulation results, our proposal significantly reduces geographic variation with only a very slight decrease in allocation efficiency as measured by transport distance and number of deaths. However, a more complete analysis would

Figure 3-3: Box Plot of Transplant MELD, by Region

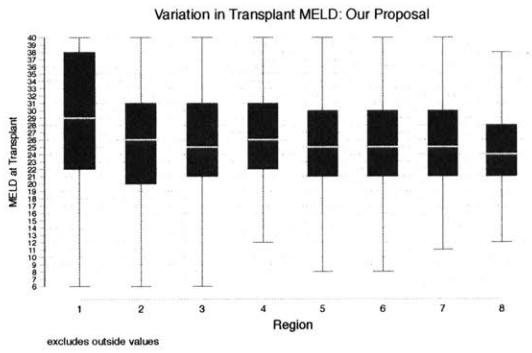

(a) Our Proposal

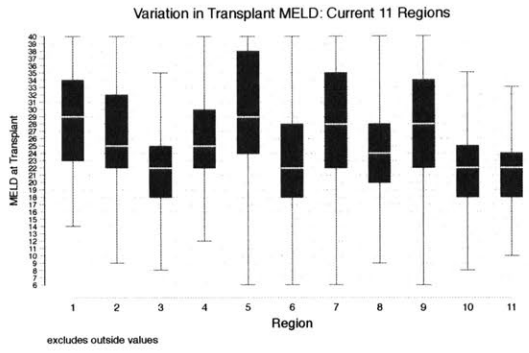

(b) Current 11 Regions

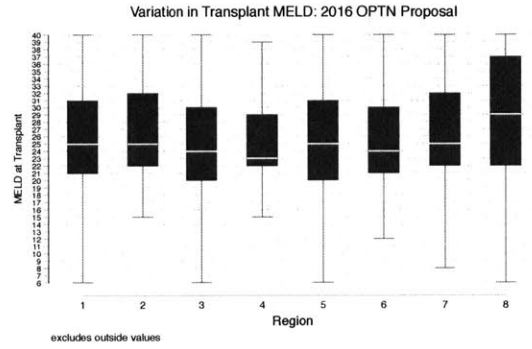

(c) 2016 OPTN Proposal

need to be performed before definitively stating one region design is superior to another. For instance, one would need to ensure that certain sub-populations are not disproportionately affected by the redistricting. A comprehensive cost analysis would also need to be performed in order to weigh financial considerations with qualitative judgments, such as fairness. With those qualifications in mind, we present this region design as a promising option that could improve the allocation system. In the following chapters, we will develop the methodology and models used to arrive at these optimized regions.

Allocation Metric	Region Design Scheme		
	8 Region Proposal	Current 11 Regions	2016 Public Comment Regions
SD of Regional Median MELD	1.59	2.95	1.77
Median Travel Time	1.68	1.63	1.66
Median Distance	120.9	105.9	118.1
Percent Organs Flown	53	51	53
Transplants	6096	6088	6130
National Transplants	247	415	282
Discarded Organs	602	610	568
Waitlist Deaths	1394	1416	1406
Total Deaths	2776	2821	2774
Median Post-Graft Life Years	5	5	5

Table 3.1: Key Simulation Results

THIS PAGE INTENTIONALLY LEFT BLANK

Chapter 4

Fluid Approximation of the Liver Allocation System

The liver allocation system is a dynamic process in which patients can enter the waitlist, change MELD states, and leave the waitlist through transplant, illness, or death. In this section, we describe a fluid model that approximates the steady state waitlist given the number of arriving patients and a MELD transition matrix. Then, we model a simplified liver allocation rule by developing a notion of 'waterfilling', in which the supply of livers is used to deplete the steady state waitlist by descending MELD score until the liver supply is exhausted. The approximation is determined to be sufficiently accurate based on a comparison with a simulation of the stochastic process.

4.1 Fluid Approximation of Candidate Waitlist

The liver allocation process is stochastic process, with randomness stemming from liver and patient arrivals, MELD progression, and the candidate's liver acceptance decision. Due its complexity, it is very difficult to tractably model the allocation process as a steady state stochastic process. Akan et al. model the liver transplant waiting list as a multiclass fluid model of overloaded queues, which captures the patients' ability to change MELD scores over time by switching classes [2]. In their

model, there are multiple classes of livers, which represent the organ's quality. Patients reject a liver based on an estimated function of static patient characteristics, which notably do not include distance to liver. Using this fluid model, the authors derive optimal policies using optimal control theory.

We adopt a simpler approach motivated by the same fluid approximation. Specifically, we produce a set of equations that dictate that the incoming flow to any MELD state is equal to the outgoing 'flow' in steady state. Let T be a 36x36 square matrix in which T_{jk} equals the probability that an individual transitions from MELD state j to k, for each of the 35 MELD states. T_{j40} represents the probability that a patient exits the waitlist from MELD j, either due to death or illness. Next, let λ_i equal the number of patients arriving into the waitlist at MELD i in one week. Let x_i represent the number of individuals in the waitlist at MELD i. For now, assume there are no livers arriving to the system and therefore no transplants. Thus, the only way in which individuals leave the system is through death or illness. Then, the fluid approximation imposes the following structure on the system:

$$\sum_{i=6, i\neq j}^{40} T_{i,j}x_i + \lambda_j = x_j(1 - T_{jj}), \text{ for all MELD } j \tag{4.1}$$

$$x_i \geq 0 \tag{4.2}$$

The left hand side of Equation[1] 4.1 represents the number of individuals entering MELD state j, and the right hand side represents the number of individuals existing. In steady state, these two flows we be equal, and the x_i will represent the numbers of individuals on the waitlist in MELD state i. Note, x_j is not indexed by a time component since this equation applies in steady state.

4.1.1 Steady State Waitlist: Simulation

This fluid model approximation removes the stochasticity from the process and instead relies on averages. Therefore, to test the approximation, we compare the results

[1]In this thesis, we use 'Equation' loosely to refer to inequalities

from the fluid model with a simulation of the stochastic system.

We define the unit of time of each event to be one week. Patients are modeled as arriving to the system at a given MELD during a period of time as a Poisson random variable with parameter λ_i. The transition between MELD i and MELD j is modeled as a multinomial random variable. The parameters for these random variables are estimated from data, as described in Chapter 5. After running the simulation for 10,000 weeks to ensure the process is in steady state, we record the number of patients at each MELD. Then, we compare the simulated distribution of individuals on the waitlist with the outcome of the fluid approximation model.

Figure 4-1: Steady State Waitlist: Fluid Appoximation (Red) vs. Simulation (Blue)

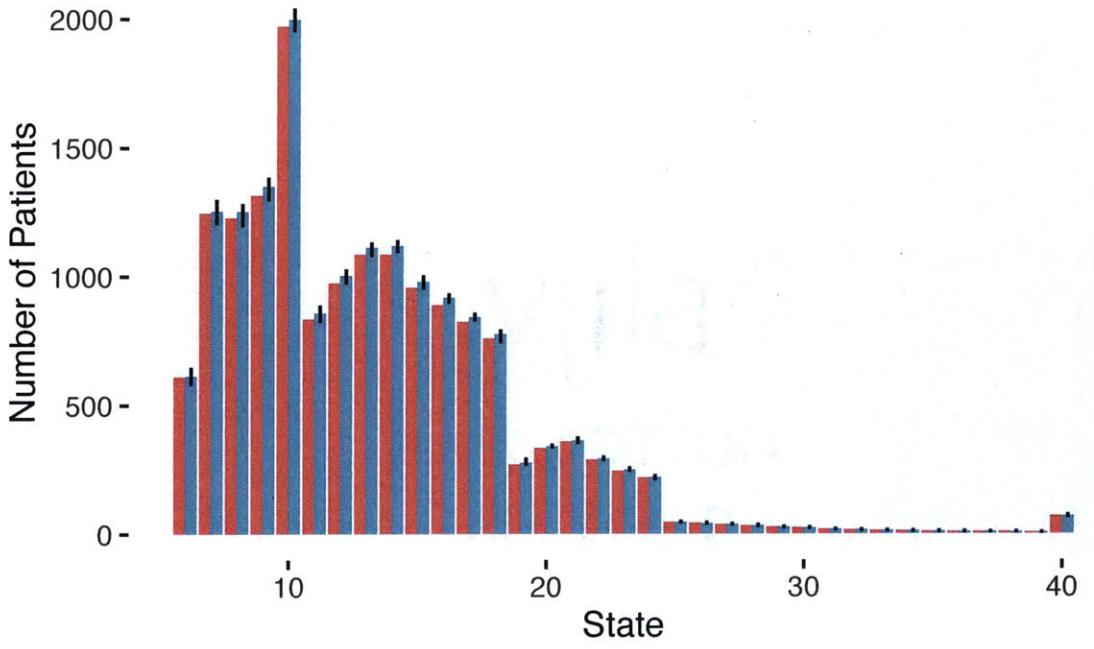

Figure 4-1 shows the comparison between the fluid approximation and the simulation. The black bar represents the range of results over 10 iterations of the simulation. The arrival parameters, λ, were estimated from the national waitlist data for year 2015. The number of patients in the waitlist never differ by more than 3% between the simulation and the fluid model. Furthermore, the key metric used by policy makers - the median MELD - is the same for both approaches. The results were also

robust to the arrival parameter, λ, and the transition matrix, T. This comparison suggests that the fluid model accurately characterizes the steady state waitlist of the liver allocation system.

4.2 Waterfilling as an Allocation Mechanism

Next, we propose a simplified model of liver allocation that can be incorporated in the fluid model. Although the allocation process depends on many factors such as blood compatibility, waiting time, and exception points, the predominant force is MELD. Therefore we propose a simplified model of allocation that depends only on MELD, within a given region. We dictate that the supply of livers depletes the steady state waitlist at the highest MELD score, then proceeds to the next highest MELD, until the supply of livers is exhausted. To incorporate this waterfilling allocation rule to the fluid approximation model, we introduce the following notation. Let u_i be the number of transplants occurring at MELD i in steady state. Next, let y_i be a binary variable equal to 1 if the steady state of waitlist at MELD i is depleted. In other words,

$$y_i = \begin{cases} 1 & x_i = 0 \\ 0 & x_i > 0 \end{cases} \tag{4.3}$$

Next, we introduce three constraints that enforce the waterfilling dynamics. Equation 4.4 constrains the number of transplants to be no greater than the supply of liver into the system, where U is the rate of incoming livers. Equation 4.5 enforces that $y_i = 1$ if and only if $x_i = 0$. Finally, equations 4.6 and 4.7 constrain the number of transplants at MELD i to be 0 unless the waiting list is depleted at MELD $i + 1$.

$$\sum_{i=6}^{40} u_i \leq U \tag{4.4}$$

$$x_i \leq (1 - y_i) \tag{4.5}$$

$$u_i \leq U y_{i+1} \tag{4.6}$$

$$y_{i+1} \geq y_i \tag{4.7}$$

Finally, we adapt Equation 4.1 to incorporate the addition of livers and transplants into the fluid model.

$$\sum_{i=6, i\neq j}^{40} T_{i,j}x_i + \lambda_j = x_j(1 - T_{jj}) + u_i, \text{ for all MELD } j \tag{4.8}$$

Like equation 4.1, the left hand of equation 4.8 represents the flow into a given state and the right hand side the flow out. But in this case, the flow out of a MELD state also includes transplants. Equations 4.5, 4.4, and 4.7 enforce the waterfilling dynamic. The supply of livers, U, is first allocated to the highest MELD and only allocated to a lower MELD if the steady state waitlist at the higher MELD is depleted. We note that there is a unique allocation of livers given a transition matrix and incoming rates.

4.2.1 Steady State Transplants: Comparison with Simulation

We extend the simulation approach from Section 4.1.1 to include the arrival of livers. Specifically, we model livers arriving to the system during a period of time as a Poisson random variable. Then, we let the simulation reach steady state by running for 10,000 weeks. We then compare the simulated steady state waitlist and the steady state transplantations with the result of the fluid approximation model.

Figure 4-2 shows the comparison of the transplants (on the left) and the waitlist (on the right). As before, the blue represents the simulation and the red the fluid model results. Each row represents a different rate of incoming livers. For instance, the first row represents 5 livers arriving per week. As the rate of liver arrivals increases, the steady state waitlist is depleted from the highest MELD states. As before, the simulation and the fluid model are reasonably similar. The approximation is within 4% of the simulated number of patients waiting at each state. There are noticeable differences between the two approaches among the transplants at the lower MELD scores. These differences can be as large as 25%, although on average the difference is less than 5%. Furthermore, the median MELD at transplant is the same for both

approaches. Therefore, the fluid model approximation is suitably accurate for our purposes.

Figure 4-2: Left: Steady State Transplant States; Right: Steady State Waitlist

(a) $U = 5$ (b) $U = 5$

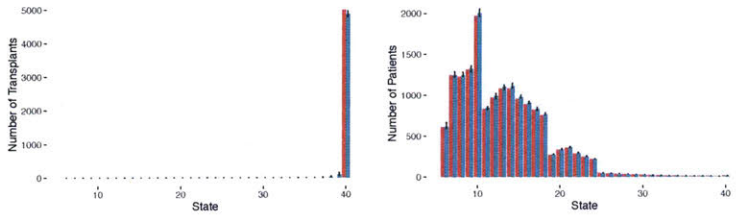

(c) $U = 10$ (d) $U = 10$

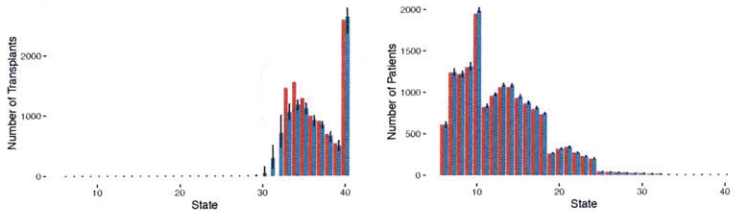

(e) $U = 15$ (f) $U = 15$

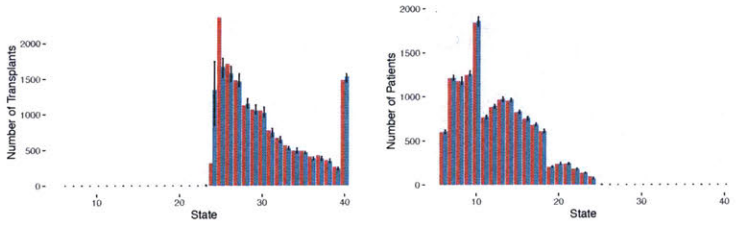

(g) $U = 20$ (h) $U = 20$

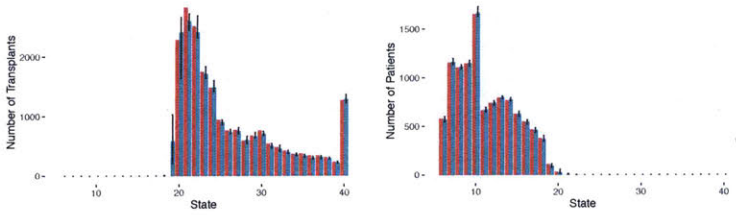

(i) $U = 25$ (j) $U = 25$

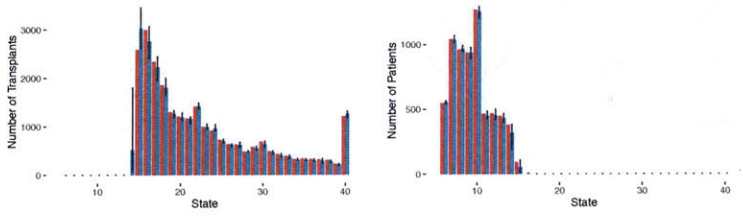

4.3 Applications

In this chapter, we proposed a fluid model of the liver allocation system that accurately approximates the true dynamics. This approach is very tractable, especially compared to any exact queuing model. The fluid model approximation and water-filling approach will be embedded directly in the optimization models, presented in Chapters 6 and 7. Although we model patients and livers as homogeneous, it is straightforward to extend the model to include multiple types of patients and livers. Beyond the application to liver allocation, this fluid model approximation might also be relevant in other domains with multi-class queues with class-switching.

THIS PAGE INTENTIONALLY LEFT BLANK

Chapter 5

Parameter Estimation

In this chapter, we discuss the parameters used in the optimization formulations in Chapters 6 and 7 and the methodology used to estimate them.

This study used data from the Scientific Registry of Transplant Recipients (SRTR). The SRTR data system includes data on all donor, wait-listed candidates, and transplant recipients in the US, submitted to the members of the Organ Procurement and Transplantation Network (OPTN). The Health Resources and Services Administration (HRSA), U.S. Department of Health and Human Services provides oversight to activities of OPTN and SRTR contractors.

5.1 Disease Progression

An accurate estimate of the MELD transition matrix is crucial to any model of the allocation system. Previous research has used cubic splines to interpolate between observed laboratory values to develop a model that can predict individual changes in MELD [3]. However, the analysis used a database of laboratory values that is not publicly available. Instead, we estimate the progression of MELD scores based on simulation results. Unlike Alagoz et al., we do not attempt to infer the trajectory of the MELD score between recorded observations. Instead, we aim to estimate the transition of recorded MELD scores for a representative patient, since the allocation system only depends on the most recently recorded MELD score.

Specifically, we are interested in the progression of MELD scores in the absence of any liver allocations. Therefore, we take advantage of the existing liver simulator, LSAM, to model this behavior. We modify the simulator to restrict all donor organs. Then, we simulate the MELD score updates between January 1st 2010 and December 31st 2010, resulting in a total of 250,000 MELD updates for over 28,000 individuals. Using this large sample of simulated results, we calculate the frequency of transitions from one MELD state to another during the span of 7 days. The resulting transition table is presented in Table A.4. Since MELD score is defined and calibrated as a mortality rate, we can compare our estimated transition matrix with the established mortality rates associated with each MELD [26]. Since the MELD scores are calibrated to 90 day mortality rates, we convert our transition matrix to the same time period by raising it to the power of $90/7 \approx 12.6$. The estimated and published 90-day mortality rates are shown in Table 5.1. Although there are minor differences between the the estimated and the calibrated mortality risks, the estimated matrix is suitably close for our purposes.

Table 5.1: Comparison of Transition with Established MELD Mortality Probabilities

MELD	Transition 90 Day Mortality	Stated 90 Day Mortality
0-9	4.3	1.9
10-19	5.5	6.0
20-29	14.1	19.6
30-39	33.0	52.6
> 40	50.9	79.3

We estimate one transition matrix using all available patient data and apply that estimated matrix to all patients in the optimization models. We note that the actual transition matrix may differ for different subgroups of patients. For instance, patients with hepatocellular carcinoma (HCC) are known to follow a different health trajectory than non-cancer patients. Future work may estimate different transition matrix for HCC vs non-HCC patients.

5.2 Distance and Travel Time Matrix

The liver transport time and distance are key metrics of efficiency in the allocation system. Therefore, we need to include accurate estimates of travel distance and time between DSAs in the optimization formulation. Since DSAs are geographic areas and not single points, we need to estimate the distance and travel times between each pair. Livers are recovered from deceased donors at donor hospitals and then transported to the transplant center that performs the transplant operation. Each DSA contains between 0 and 6 transplant centers. Therefore, to estimate the distance between DSA j and DSA k, we calculate the mean pairwise distance between donor hospitals in DSA j and the transplant hospitals in DSA k, weighted by the number of transplants at each center in DSA k. Specifically, the transplant weighted distance between the DSA j and DSA k, T_{jk}, is as follows:

$$D_{jk} = \sum_{(T,H)\in P_{jk}} \left(\frac{t_T}{t_k}\right) d_{TH} + \sum_{(T,H)\in P_{kj}} \left(\frac{t_T}{t_k}\right) d_{TH} \tag{5.1}$$

where P_{jk} is the set of transplant centers (T) in DSA j and donor hospitals (H) in DSA k, t_T is the number of transplants in transplant center T, t_k is the total number of transplants in DSA k, and d_{TH} is the distance between transplant hospital T and donor hospital H.

Using a similar approach, we estimate the travel time between each pair of DSAs.

$$TT_{jk} = \sum_{(T,H)\in P_{jk}} \left(\frac{t_T}{t_k}\right) \tau_{TH} + \sum_{(T,H)\in P_{kj}} \left(\frac{t_T}{t_k}\right) \tau_{TH} \tag{5.2}$$

where τ_{TH} is the estimated travel time between transplant hospital T and donor hospital H. The estimates for τ_{TH} were provided by the Liver Simulation Allocation Model and were developed by Gentry et. al [11]. The estimates are based on a model with three transport modes - car, helicopter, and plane - that incorporate distances to the nearest airport and estimated flight time.

5.3 Contiguity Constraints

OPTN requires that all regions be contiguous. Since the success of the transplant is inversely related to the time the organ must travel before transplantation, non-contiguous regions would likely result in an inefficient system since travel times would increase. Furthermore, non-contiguous would pose operational problems for the organizations responsible for allocating livers. Therefore, we impose constraints on the optimization model that ensure contiguous regions.

There are multiple ways to formulate contiguity constraints. First, one could use a location-allocation formulation, which finds a set of reference nodes (region centers), such that when each DSA is assigned to the nearest reference node, some objective is achieved. By enforcing that each DSA be assigned to the closest region center, the resulting regions are almost always contiguous [6]. However, this formulation also eliminates many contiguous regions. This formulation is used in the work of Gentry et al. that contributed to the 2016 OPTN redistricting proposal [14].

Shirabe, on the other hand, introduced a clever formulation of exact contiguity that needs only a linear number of constraints [22]. In this formulation, each node receives one unit of flow. A region is contiguous if and only if there exists one DSA that acts as a sink and receives one unit of flow from all other DSAs in the region, where flow can only travel between adjacent DSAs.

A simpler approach requires that each region is a a subtree of a shortest path subtree rooted at the regions center [1]. For each DSA k of region r, at least one of the adjacent DSAs $j \in N(k)$ that immediately precedes k on some shortest path to the center of the region also has to be included in region r. If we define $S_k = \{j \in N(k) | \text{j immediately precedes } k \text{ on some shortest path to } c_k\}$, then we can write the contiguity constraints as follows:

$$w_{kr} \leq \sum_{j \in S(k)} w_{jr} \text{ for all DSA k and region } r \tag{5.3}$$

where w_{kr} is a binary decision variable equal to one if DSA k is assigned to region r [1]. This formulation does exclude some regions, but those regions tend to have odd

shapes, such as large protrusions or extensions. Unlike the location-allocation constraint, the center of a region does not have the same interpretation as the geographical center, allowing greater flexibility. This formulation has significant computational advantages. Therefore, we use this approach to model contiguity constraints in our optimization formulation.

To implement this formulation, we construct the adjacency matrix based on the DSAs. With this adjacency matrix established, it is straightforward to calculate the shortest path between each pair of DSAs, which will be used in the contiguity constraints. In this case, the link costs were the estimated travel time between each pair of DSAs.

With this adjacency matrix established, it is straightforward to calculate the shortest path between each pair of DSAs, which will be used in the contiguity constraints. In this case, the link costs were the estimated travel time between each pair of DSAs.

5.4 Initial Regions

Due to computational restrictions, we impose a heuristic on the region design. We predesignate 8 DSAs to each serve as a reference node for one of the 8 regions. In any region configuration, each DSA must have a contiguous path to the region's reference node. Therefore, by assigning these reference nodes, we are restricting that two reference nodes can never be in the same region. Therefore, we select the 8 reference nodes that are maximally far apart. Specifically, we solve the following optimization problem that maximizes the minimum distance between any two DSAs. The resulting starting regions are shown in Figure 5-1.

5.4.1 Initial Region Optimization Formulation

Let c_k be the binary variable equal to 1 if DSA k serves as a reference node for one of the eight regions. Let d correspond to the minimum distance between any two reference nodes. Equation 5.8 requires d to be greater than the distance between any two reference nodes and equation 5.7 dictates that there are exactly 8 reference

nodes. Then, the objective function is simply to maximize d, the minimum distance between reference nodes.

Decision Variables

$$c_k = \begin{cases} 1 & \text{DSA k is a reference node} \\ 0 & \text{otherwise} \end{cases} \tag{5.4}$$

$$d = \text{Minimum distance between two reference nodes} \tag{5.5}$$

Data

$$D_{jk} = \text{ Distance between DSA } j \text{ and } k \tag{5.6}$$

Constraints

$$\sum_k c_k = 8 \tag{5.7}$$

$$d \leq D_{jk} + M(2 - c_k - c_j) \text{ for all DSA j and k} \tag{5.8}$$

Objective

$$\max d \tag{5.9}$$

Figure 5-1: Starting Regions

This heuristic provides substantial computational improvement, allowing us to include other important aspects of the allocation process in the optimization formulation. Furthermore, the heuristic does not seem to significantly affect optimal

Year	Baseline		Starting Heuristic	
	Objective	Run Time (s)	Objective	Run Time (s)
2010	454	1473	492	59
2011	212	841	264	97
2012	160	1473	114	129
2013	128	1412	90	144
2014	106	718	180	71
2015	112	1473	112	80

Table 5.2: Effect of Starting Region Heuristic on Run Time and Optimality: 3 Hour Travel Time Max

solutions. To gauge the effect of this heuristic on both computational run time and optimal results, we run an optimization formulation with and without the heuristic. Specifically, we consider the formulation that minimizes the absolute sum of regional differences in rates of supply and demand, described in Chapter 1. This formulation, which was the foundation of the 2016 OPTN redistricting proposal, uses a location-allocation formulation, which simultaneously selects the centers and the regions. Table 5.2 compares both the objective value and the run time for the baseline formulation and our heuristic.

This test case indicates that the performance of our heuristic is comparable to location-allocation approach. In some cases, our approach actually achieves a lower objective value, corresponding to a smaller absolute difference in supply and demand across regions. Although the baseline model allows the centers of regions to to be defined more flexibly, it excludes many contiguous regions. Our heuristic, even though it has some imposed spatial structure, only requires regions be contiguous, thereby resulting in a greater set of feasible regions. The heuristic provides optimal solutions significantly faster than the location-allocation formulation. In some instances, the difference in computation time is ten-fold.

5.5 Liver and Patient Arrivals

Lastly, we estimate the number of liver arrivals and patient arrivals at each OPO. For each year between 2011 and 2015, we estimate yearly liver arrival rates from the

SRTR data. Similarly, we calculate the number of individuals joining the waitlist at each MELD in each DSA. Due to difference in listing low-MELD patients, there are significant differences in the distribution of MELD score for patients entering the waitlist across DSAs. Table A.1 shows that the median MELD at the time of registration can vary significantly. Therefore, by modeling arrivals into each MELD state we capture a more precise measure of demand.

Chapter 6

Model 1: Minimization of Variation in Median MELD

In this chapter, we incorporate the fluid approximation of the allocation system and the estimated parameters to formulate the first of two models aimed at reducing geographic inequity. Due to computational limits, it was not possible to include all the desired modeling choices in a single model. Therefore, we propose two complementary models that approach reducing geographic variation from slightly different angles. Both formulations focus on the case with 8 regions, as the 2016 proposal uses 8 regions. However, the formulations and methodology can be trivially extended to any number of regions.

Recall from Chapter 1 that the liver allocation system has two, often competing, objectives. The livers should be allocated to those with the greatest need, but the efficiency of the overall system should be maintained by reducing the liver transportation distances. Therefore, this chapter proposes a model that directly models and minimizes the variation in the median transplant MELD across the regions, which is the key metric of geographic variation identified by OPTN [18]. Then, to constrain the degree to which livers are transported long distances, we impose a limit on the maximum travel time within each region. We show that although the model effectively reduces the geographic variation, it results in increased median liver transport times and distances. The simulation results are used to motivate the second model,

presented in Chapter 7, which directly minimizes the total liver distance and travel time instead of simply imposing a constraint on region size.

6.1 Formulation

This section defines the input data, decision variables, and constraints used in the model.

Data

The model has several parameters estimated from the waiting list and transplant data, as described in 5. Equations 6.1 through 6.6 introduce the MELD transition matrix, incoming patients, incoming livers, travel time matrix, and the number of hospitals in each DSA. $A_j(c)$ represents the shortest path from DSA j to center c, as introduced in Equation 6.7.

$$T_{ij} = \text{ probability of transitioning from MELD } i \text{ to } j \text{ in 1 week} \tag{6.1}$$

$$\lambda_{ki} = \text{ Number of patient arrivals to DSA } k \text{ at MELD } i \text{ in 1 week} \tag{6.2}$$

$$U_k = \text{ Number of livers arriving at DSA } k \text{ in 1 week} \tag{6.3}$$

$$TT_{jk} = \text{Travel time (hours) between DSAs } j \text{ and } k \tag{6.4}$$

$$H_j = \text{Number of transplant hospitals in service area of OPO } j \tag{6.5}$$

$$C_r = \text{Reference node of region } r \tag{6.6}$$

$$A_j(c) = \text{The set of DSAs directly preceding } j \text{ on the shortest path from } j \text{ to } c \tag{6.7}$$

Decision Variables

This model is akin to a districting problem in which we group geographical units together to achieve a certain objective. In this case, equation 6.8 introduces the key decision variable, w_{jr}, which assigns each DSA j to a region r. Equations 6.9, 6.10, and 6.11 introduce the decision variables corresponding to the waiting list, transplants, and depletion state indicator as described in 5. Equations 6.12 and 6.13 introduce decision variables used to model the median MELD at transplant within each region.

$$w_{jr} = \begin{cases} 1 & \text{DSA } j \text{ is in region } r \\ 0 & \text{otherwise} \end{cases} \tag{6.8}$$

$$x_{jr} = \text{ Number of patients waiting at MELD } j \text{ in region } r \tag{6.9}$$

$$u_{ir} = \text{ Number of transplants at MELD } i \text{ in region } r \tag{6.10}$$

$$y_{ir} = \begin{cases} 1 & x_{jk} = 0 \\ 0 & x_{jk} > 0 \end{cases} \tag{6.11}$$

$$h_{ir} = \begin{cases} 1 & \text{MELD } i \text{ is greater than the median MELD in region } r \\ 0 & \text{Otherwise} \end{cases} \tag{6.12}$$

$$m_r = \text{Median MELD score at transplant for region } r \tag{6.13}$$

Constraints

Median Constraint

Next, we introduce constraints to model median MELD. First, equations 6.14, 6.15, and 6.16 require that h is an increasing binary sequence according to MELD scores for each region. Next, we note that the median for a given region, m_r corresponds to the MELD, m, such that the absolute difference between the sum of transplants at MELD less than m and the sum of transplants greater than m is less than the number of transplants at MELD m. Eqn 6.17 imposes this median constraint for each MELD. However, the right hand side of the constraint also includes a term that effectively removes this constraint for all MELD i that are not chosen to be the median. Therefore, the median constraint will only apply when $h_{ir} = 0$ and $h_{i+1,r} = 1$. Then, we can model the median MELD for each region r using 6.18. This formulation is motivated by the Bertsimas-Stock model, which has shown to be much computationally tractable than alternative formulations [5].

$$h_{6k} = 0 \tag{6.14}$$

$$h_{40k} = 1 \tag{6.15}$$

$$h_{i+1,r} \geq h_{ir} \tag{6.16}$$

$$\left| \sum_{j=6}^{i-1} u_{jr} - \sum_{j=i+1}^{40} u_{jr} \right| \leq u_{ir} + M(1 - h_{i+1,r} + h_{ir}) \tag{6.17}$$

$$m_r = \sum_{i=6}^{40} i(h_{i+1,r} - h_{ir}) \text{ for every region } r \tag{6.18}$$

Policy Constraint

Next, we impose constraints dictated by OPTN policy guidelines. Equation 6.19 requires any region to have at least 6 transplant centers, which effectively puts a lower bound on the allowable size of any region. Equation 6.20 puts an upper bound on the region size, by constraining any DSA to be within a certain travel time from the region's reference node. The allowable travel time, τ, is a model parameter.

$$\sum_{j=1}^{58} w_{ir} H_j \leq 6 \text{ for every region } r \tag{6.19}$$

$$w_{jr} TT_{j,C_r} <= \tau \text{ for every DSA } j \text{ and region } r \tag{6.20}$$

$$\sum_{r=1}^{58} w_{jr} = 1, \text{ for all DSA } j \tag{6.21}$$

Fluid Approximation Constraints

Next, we impose the fluid model and waterfilling constraints that approximate the dynamics of the allocation process. Equation 6.22 constrains the number of a transplants in a region to be equal to the number of livers arriving into the system. Therefore, in this model, no livers are transplanted outside of the region. In 2015, approximately 7% of livers were transplanted outside of the region in which they were recovered. Therefore, although this is a simplification of the system, restricting livers to be transplanted within a region still captures the majority of the transplants.

Equation 6.23 dictates the flow of patients into a given MELD state to be equal to the flow out, and equations 6.24, 6.25, 6.26 enforce the 'waterfilling' liver allocation approximation. As described in Chapter 4, the waterfilling approach assumes that the liver is always allocated to the candidate with the highest MELD. We implicitly assume that every candidate accepts the liver when offered. However, in reality, candidates often reject a liver due to many factors, including the quality of the liver and the distance it has to travel. By assuming that candidates always accept a liver,

we are significantly simplifying the allocation system.

$$\sum_{i=1}^{58} u_{ir} = \sum_{j=1}^{58} w_{jr} U_j \text{ for every region } r \tag{6.22}$$

$$\sum_{i=1, i\neq j}^{58} T_{i,j} x_{i,k} + \sum_{d=1}^{58} \lambda_{d,j} w_{d,k} = u_{j,r} + x_{jk}(1 - T_{jj}) \text{ for all region } r \text{ and MELD } j \tag{6.23}$$

$$x_{ir} \leq M(1 - y_{ir}) \text{ for all MELD } i \text{ and region } r \tag{6.24}$$

$$u_{ir} \leq M y_{i+1,r} \text{ for all MELD } i \text{ and region } r \tag{6.25}$$

$$y_{i+1,r} \geq y_{ir} \text{ for all MELD } i \text{ and region } r \tag{6.26}$$

Contiguity Constraints

Equation 6.27 enforces the regions be contiguous, as described in Chapter 5.

$$w_{kr} \leq \sum_{j \in A_k(c_r)} w_{jr} \tag{6.27}$$

Objective

Finally, the objective minimizes the variation in median MELD at the time of transplant across the regions. Specifically, equation 6.28 minimizes the sum of absolute differences between the median at region r and the mean median MELD.

$$\min \sum_{k=1}^{58} \left| m_r - \frac{\sum_{j=1}^{8} m_j}{8} \right| \tag{6.28}$$

6.2 Results

Next, we present the simulation results for the optimized regions when the travel time limit, τ is 3 and 4 hours. Furthermore, as a robustness check, we present the results based on input data for each year from 2011-2015. The simulation results are all based on 2010. Tables 6.1a and 6.1b summarizes the key metrics for the model with 3 and 4 hour travel times, respectively. Furthermore, we present a baseline model that minimizes the sum of absolute regional differences in rates of supply and demand, as described in Chapter 1. We present the results of the baseline with both a 3 hour and 4 hour constraint on travel time to the region center. Tables 6.2a and 6.2b present the results of this baseline approach. Lastly, we recall the results of the current region configuration and the 2016 OPTN proposal presented in 3.1.

6.3 Discussion

For the 3 hour travel time case, the standard deviation of median MELD ranges from 2.20 to 3.04, depending on the year of input data. Similarly, the 4 hour travel time produces values in the range of 2.19 and 2.87. Compared to the current system, which has a standard deviation in median MELD of nearly 3, our approach reduces geographic variation in almost all cases. However, since the current approach has 11 regions and our approach considers 8 regions, the median transport distance and time increase substantially under approach. However, as a result of the reducing the geographic variation, some other key metrics of efficiency have improved, such as number of transplants, discarded organs, and total deaths. Therefore, the optimized regions generally outperform the current region configuration, except for transport time and distance.

However, compared to the 2016 OPTN proposal, the results are not quite as favorable. Our model often results in geographic variation greater than that of the proposal. Furthermore, our model also often results in greater transport times and distances. With regard to other key efficiency metrics, the results are quite similar.

Table 6.1: Simulation Results: Minimization Variation MELD Model

Metric	Data Input Year 2011	2012	2013	2014	2015
SD of Median Regional Transplant MELD	2.20	2.67	2.88	3.04	2.51
Median Travel Time (Hours)	1.72	1.70	1.74	1.72	1.72
Median Distance (Miles)	141.06	128.72	143.50	137.40	137.18
Percent Organs Flown	55%	54%	56%	55%	55%
Discarded Organs	582	577	573	556	555
Median Wait for Graft (Days)	89.9	87.2	88	89.7	92
Transplanted Organs	6116	6121	6125	6142	6143
Local Transplants	3,545	3,538	3,478	3,523	3,549
Regional Transplants	2,286	2,275	2,290	2,315	2,328
National Transplants	285	308	357	304	266
Total Deaths	2,782	2,762	2,765	2,776	2,761
Waitlist Deaths	1,396	1,383	1,392	1,395	1,365
Post-Graft Surviving	5,317	5,317	5,299	5,337	5,338

(a) 3 Hour Travel Time Constraint

Metric	Data Input Year 2011	2012	2013	2014	2015
SD of Median Regional Transplant MELD	2.87	2.19	2.45	2.90	2.15
Median Travel Time (Hours)	1.73	1.71	1.70	1.69	1.70
Median Distance (Miles)	138.4	135.7	123.6	127.6	121.4
Percent Organs Flown	55%	55%	54%	54%	53%
Discarded Organs	616	585	585	573	592
Median Wait for Graft (Days)	85	91	91.8	88.8	92.3
Transplanted Organs	6082	6113	6113	6125	6106
Local Transplants	3,449	3,577	3,580	3,573	3,557
Regional Transplants	2,348	2,271	2,247	2,204	2,280
National Transplants	285	265	286	348	269
Total Deaths	2,776	2,800	2,812	2,800	2,727
Waitlist Deaths	1,376	1,399	1,428	1,404	1,379
Post-Graft Surviving	5,263	5,286	5,311	5,301	5,365

(b) 4 Hour Travel Time Constraint

The number of deaths, transplants, and median-days awaiting transplantation are all comparable between the two models. Therefore, the 2016 proposal seems to dominate our model in regard to geographic variation and median transport distance.

Lastly, we note that our model produces comparable results to the baseline. Both models produce similar metrics of geographic variation, distance, and efficiency. Furthermore, we both models are sensitive the the year of input data, as indicated by

Table 6.2: Simulation Results: Baseline Model

	Input Year				
Metric	2011	2012	2013	2014	2015
SD of Regional Median Transplant MELD	2.47	2.59	2.25	2.98	2.83
Median Time (Hours)	1.70	1.70	1.70	1.70	1.67
Median Distance (Miles)	131.2	133.8	134.3	123.6	116.7
Percent Organs Flown	55	55	55	54	52
Discarded Organs	620	601	632	583	632
Median Days Wait For Graft	86.2	91	84	88.7	83.9
Transplanted Organs	6,078	6,097	6,066	6,115	6,066
Local Transplants	3,530	3,472	3,419	3,559	3,577
Regional Transplants	2,240	2,276	2,322	2,304	2,207
National Transplants	308	349	325	252	282
Total Deaths	2,743	2,750	2,789	2,790	2,757
Waitlist Deaths	1,395	1,379	1,404	1,398	1,384
Median Post-Graft Life-Years	5	5	5	5	5

(a) 3 Hour Travel Time Max

	Input Year				
Metric	2011	2012	2013	2014	2015
SD of Regional Median Transplant MELD	1.92	1.98	2.23	2.47	2.19
Median Time (Hours)	1.69	1.71	1.70	1.68	1.70
Median Distance (Miles)	122.8	134.9	137.0	118.1	131.2
Percent Organs Flown	54	55	55	53	54
Discarded Organs	591	590	583	614	588
Median Days Wait For Graft	89.2	84	90	85.1	85.9
Transplanted Organs	6,107	6,108	6,115	6,084	6,110
Local Transplants	3,591	3,494	3,478	3,525	3,502
Regional Transplants	2,221	2,300	2,304	2,276	2,259
National Transplants	295	314	333	283	349
Total Deaths	2,809	2,804	2,775	2,814	2,785
Waitlist Deaths	1,426	1,415	1,388	1,402	1374
Median Post-Graft Life-Years	5	5	5	5	5

(b) 4 Hour Travel Time Max

the large ranges in key metrics across the years.

Based on these results, our model seems to be inadequately constraining the region size. Interestingly, increasing the limit on within-region travel time in the optimization did not necessarily produce regions that resulted in larger median transport times or times. In fact, in many instances, the regions actually had a significantly lower median transport time. Other metrics of liver allocation efficiency, such as total

deaths and number of transplants, are relatively similar for our approach and the 2016 proposal. Therefore, it seems that constraints on the region size are not an effective modeling approach to limit the distances the livers travel. One possible explanation for this phenomenon is that even though we constraint the region size, we are not considering how livers being geographically allocated within a region. In the next chapter, we address this issue by formulating a model that captures the flows of livers between any two OPOs, and therefore allows us to minimize the total distance.

Chapter 7

Model 2: Minimization of Total Liver Transport Time

The previous model directly minimized the variation in median MELD at transplant across regions, but did not explicitly capture the flows of organs from one geographic area to another. However, as discussed in Chapter 1, the efficiency of the liver allocation system depends on livers traveling short distances between donors and recipients. The simulation results indicate that the median distance traveled was significantly higher than both the existing allocation scheme and alternative proposals, indicating a relatively inefficient allocation system. Therefore, in this section, we formulate a model which minimizes the total amount of time it takes to ship the livers, given some acceptable level of geographic variation.

7.1 Model Motivation

In this model, we aim to find regions that minimize the liver transport time between donor hospitals and transplant hospitals, subject to a certain allowable geographic variation. To motivate this approach, consider a hypothetical region with 5 OPOs in Figure 7-1. Let TT_{jk} be the time it takes to transport an organ from within DSA j to DSA k. In the optimization model, the waitlist dynamic and allocation process is approximated by the fluid model described in Chapter 4. Therefore, let s_{kj} be the

number of livers that are recovered in DSA k and transplanted in DSA j (in a given time period) that are consistent with the modeled allocation process. Figure 7-1a presents a hypothetical example, where livers 'flow' from OPO 1 to 2, 3 to 2, and 5 to 4. In the figure, these flows are represented as arrows from the corresponding OPOs. Therefore, the model assumes that there are no organ shipments between the OPOs without an arrow. The goal in this formulation is to find regions that minimize the volume-weighted travel time of the livers. For this one-region hypothetical example, the objective would be to minimize $\sum_{jk} s_{jk}TT_{jk} = s_{12}TT_{12} + s_{23}TT + s_{54}TT_{54}$.

However, the fluid approximation of the allocation system ignores the stochasticity, and instead balances the incoming and outgoing flows of patients and organs. While this provides a good approximation of the steady state waitlist and transplants, it ignores the randomness involved in patient and liver arrivals that affects the allocation system. For instance, even if each OPO in Figure 7-1 had the same mean number of livers and patient arrivals per period of time, there would still be transplants recovered in one DSA and transplanted in another due to the stochasticity of arrival of livers and patients. In our hypothetical example in Figure 7-1, the flows between OPOs would be non-zero for all pairs. However, our model ignores stochasticity and does not capture flows between those OPOs, therefore underestimating the degree to which livers are shipped from one DSA to another.

To remedy the underestimate of organ flows, we augment our optimization problem to take into account the region size. We note that since there will be non-zero flow of livers between any two OPOs in a region due to stochasticity, larger regions will tend to have larger distances and travel times. Therefore, in the absence of a model that captures these flows, we impose a penalty on the overall region size. We formulate the region-size penalty as the sum of the travel time between each pair of links, as shown in Figure 7-1b. Therefore, the region size penalty will increase due to more OPOs being in a region, as well as OPOs being geographically far apart within a region. The penalty on the region size will be governed by a model parameter that trades off the region size with the volume-weighted liver travel time. In the following section, we formalize this idea in an optimization formulation.

7.2 Computational Considerations

As described in Chapter 6, the variation in regional median transplant MELD is a particularly relevant metric of geographic inequality. However, it was not computationally possible to model the flows of livers from one DSA to another together with the median constraints, due to the large number of variables needed to model the median. Therefore, we use a substantially simpler metric of geographic variation, which captures the supply and demand differentials that drive geographic inequity. Specifically, we model geographic disparity as the difference between actual supply and the ideal supply if there were no geographic constraints in the allocation process, as introduced by Gentry et al. [14].

Furthermore, we use aggregated MELD states in order to ease the computational burden. We aggregate all MELD states below 15, MELD scores between 16 and 20, and then each pair of MELD scores over 20. Candidates with MELD below 15 are fairly healthy and generally would not receive any benefit from a liver transplant even if an organ were offered [14]. Moreover, due to the fact that there is an imbalance between liver supply and demand, it is very improbable that a an organ would be offered to such a low MELD state under any reasonable allocation scheme. MELDs between 15 and 20 are aggregated into one state due to their relatively low occurrences of transplant. Finally, since adjacent MELD states face similar mortality risk, MELD states above 20 are aggregated into pairs of two in order to capture the key elements of disease progression, while reducing the number of variables and constraints in the model. The aggregated 13 by 13 transition matrix, T, is shown in A.5, where the $T_{i,13}$ is the transition from state i to death or waitlist removal.

7.3 Formulation

Data

The transition matrix, liver arrivals, and patient arrivals are the same as in the previous model. We introduce two new data inputs, OPO liver supply (Eqn 7.5) and

Figure 7-1: Organ Flow Schematic

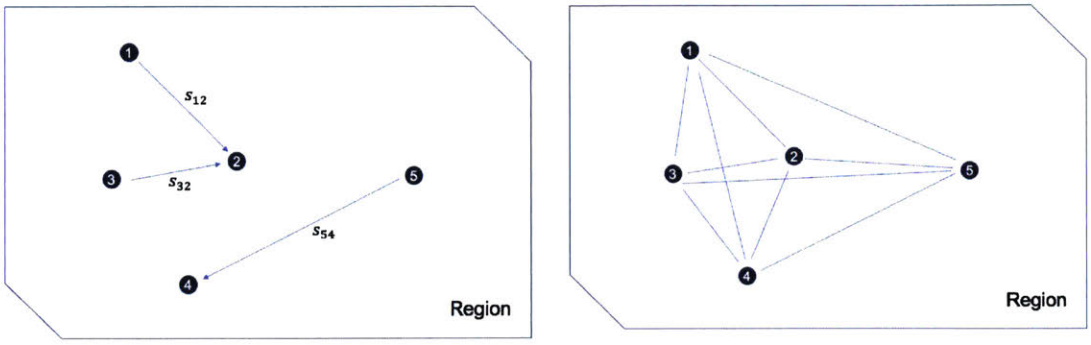

(a) Organ Flow

(b) Region Size

OPO ideal demand (Eqn 6.3).

The ideal demand, I_k, was introduced by Gentry et al. as an estimate of the number of livers that would have been transplanted in DSA k if livers were allocated entirely on MELD (without any geographic boundaries) [14]. To calculate this estimate, you consider all patients who registered on a waitlist in a given year and record the highest MELD over that time period. Then after ranking all the patients by descending MELD, the total (national) supply of livers is allocated to candidates based on their highest MELD, regardless of geographical location. I_k is the number of transplants that occurred in DSA k in this process. Since the wait list and liver arrivals are inherently dynamic, this is just an approximation of an ideal demand. However, this estimate for demand might be more preferable to other metrics, such as number of patients entering the wait list in a given time period, since it is less sensitive to differences in patient registration processes across DSAs.

$$T_{ij} = \text{ probability of transitioning from MELD } i \text{ to } j \text{ in 1 week} \tag{7.1}$$

$$I_k = \text{Number of ideal livers in DSA } k \text{ in a year} \tag{7.2}$$

$$S_k = \text{Number of transplanted livers in DSA } k \text{ in a year} \tag{7.3}$$

$$\lambda_{k,i} = \text{Number of patient arrivals at DSA } k \text{ at MELD } i \text{ in 1 week} \quad (7.4)$$

$$U_k = \text{ Number of livers arriving at DSA } k \text{ in 1 week} \quad (7.5)$$

$$TT_{jk} = \text{Travel time (hours) between DSA } j \text{ and DSA } k \quad (7.6)$$

$$H_j = \text{Number of transplant hospitals in service area of OPO } j \quad (7.7)$$

$$A_j(c) = \text{The set of DSAs directly preceding j on the shortest path from } j \text{ to } c \quad (7.8)$$

Parameters

In this model, we introduce two model parameters. First, we let K be the allowable geographic variation defined by the absolute difference between liver supply and the number of transplants in the absence of geographical constraints. Therefore, unlike the previous model, we are not directly minimizing the geographic variation, but constraining to be below some level, K. Furthermore, we define a parameter V, which governs the tradeoff between the two components of the objective function, the volume-weighted travel time and the metric of total region size.

$$K = \text{ Maximum allowable number of misdirected livers} \quad (7.9)$$

$$V = \text{ Penalty parameter on total region size} \quad (7.10)$$

Decision Variables

As in the previous model, we let w_{jr} be a binary variable that equals 1 if DSA j is assigned to region r. Equation 7.12 defines a decision variable corresponding to the number of livers that are recovered in one DSA and transplanted in another. As before, we define variables to model the number of patients in each waitlist (Eqn. 7.13, transplants (Eqn. 7.15), and whether the waitlist is depleted (Eqn. 7.14). Furthermore, Equation 7.16 defines sr_{jkr} to be a binary variable equal to 1 if both DSA j and k are assigned to the region r.

$$w_{jr} = \begin{cases} 1 & \text{DSA } j \text{ is in region } r \\ 0 & \text{otherwise} \end{cases} \tag{7.11}$$

$$s_{kj} = \text{ Number of livers recovered in DSA } k \text{ and transplanted in DSA } j \tag{7.12}$$

$$x_{ik} = \text{ Number of patients waiting at MELD } i \text{ in DSA } k \tag{7.13}$$

$$y_{ir} = \begin{cases} 1 & x_{ij} = 0 \text{ for every DSA } j \text{ in region } r \\ 0 & x_{ij} > 0 \text{ for some DSA } j \text{ in region } r \end{cases} \tag{7.14}$$

$$u_{ikr} = \text{Number of transplants at MELD } i \text{ in DSA } k \text{ in region } r \tag{7.15}$$

$$sr_{jkr} = \begin{cases} 1 & \text{DSA } j \text{ and } k \text{ are in region } r \\ 0 & \text{otherwise} \end{cases} \tag{7.16}$$

Constraints

Policy Constraints

As in the previous model, we require that each region contain 6 transplant centers.

$$\sum_{j=1}^{R} w_{jr} H_j \geq 6 \text{ for every region r} \tag{7.17}$$

$$\sum_{r=1}^{R} w_{jr} = 1, \forall \text{ OPO } j \tag{7.18}$$

Fluid Model and Waterfilling Constraints

In this section, we extend the fluid model and waterfilling constraints. Equations 7.19 and 7.20 simply enforce the relationship defined in Equation 7.16. Equations 7.21, 7.22, 7.23, 7.24 require that livers can only be transplanted within the region and that there cannot be more transplants than available livers. Equation 7.25 enforces the balance relationship that incoming patients must equal outgoing patients at each MELD state for each OPO. Lastly, equations 7.26, 7.27, and 7.28 enforce the waterfilling constraints which approximate the allocation of livers.

$$sr_{jkr} \leq w_{kr} \text{ for all DSA } j, k \text{ and region } r \tag{7.19}$$

$$sr_{jkr} \leq w_{jr} \text{ for all DSA } j, k \text{ and region } r \tag{7.20}$$

$$u_{ikr} \leq M w_{kr} \text{ for all MELD } i, \text{ DSA } j \text{ and } k \tag{7.21}$$

$$s_{jk} \leq M \sum_{r} sr_{jkr} \text{ for all DSA } j \text{ and } k \tag{7.22}$$

$$\sum_{j} s_{kj} = U_k \text{ for all DSA } k \tag{7.23}$$

$$\sum_{i,r} u_{ikr} = \sum_{j} s_{jk} \text{ for all DSA } k \tag{7.24}$$

$$\sum_{i=6, i\neq j}^{40} T_{i,j} x_{ik} + \lambda_{kj} = \sum_{r=1}^{8} u_{jkr} + x_{jk}(1 - T_{jj}), \text{ for all region } r \text{ and MELD } j \tag{7.25}$$

$$x_{ik} \leq M(2 - y_{ir} - w_{kr}) \text{ for all MELD } i \text{ and DSA } k \tag{7.26}$$

$$y_{i+1,r} \geq y_{ir} \text{ for all MELD } i \text{ and region } r \tag{7.27}$$

$$u_{ikr} \leq M y_{i+1,r} \text{ for all MELD } i, \text{ DSA } k, \text{ and region } r \tag{7.28}$$

Geographic Variation Constraint

Equation 7.29 constrains the variation in difference between supply and demand to be within some allowable range, governed by parameter K.

$$\sum_{r=1}^{8} \left| \sum_{k=1}^{58} w_{kr}(I_k - S_k) \right| \leq K \tag{7.29}$$

Contiguity Constraints

As in the previous model, we enforce the regions be contiguous, as described in Chapter 5.

$$w_{kr} \leq \sum_{j \in A_k(c_r)} w_{jr} \tag{7.30}$$

Objective

Lastly, we define the objective to be the minimization of the sum of the volume-weighted travel time of all livers and the total region size. Model parameter V governs

the tradeoff between the two components of the objective. When $V = 0$, the penalty for region size disappears and the objective is simply the minimization of volume-weighted distance.

$$\min_{j,k} \sum s_{jk} d_{jk} + V \sum_{k,j,r} sr_{jkr} TT_{jk} \tag{7.31}$$

7.4 Results

This formulation has two model parameters: K, the degree of allowable geographic variation, and V, the penalty on region size. In this section, we report the optimization and simulation results for various values of K and V. The values for K were chosen to allow for different levels of allowable geographic variation. Recall from Table 5.2, the minimum level of geographic variation, as measured as the absolute sum of differences in supply and demand across regions, ranges between 90 and 500 across the different input years. Therefore, we include values of K to allow for geographic variation above that minimum amount. Similarly, a wide range of values of V were chosen such that the problem varies between minimizing total liver transport time ($V = 0$) and minimizing total region size ($V = 100$). Table A.6 reports the full results of the optimization and simulation for $K \in \{400, 500, 600\}$ and $V \in \{0, 1, 3, 5, 7, 10, 100\}$ for input years 2010 through 2015. Due to the large number of optimization problems required to solve, we set the optimality gap at 2%.

7.4.1 Relationships between Model Parameters

Effect of Region Size Penalty (V)

As expected, when the region size parameter, V, is zero, the overall region size can be quite large. With no region size penalty, the mean of the median distances is equal to 128, and in some cases it is as high as 135. These results are considerably higher than the median distance of 106 for the current region configuration and 118 for the 2016 OPTN proposal. We attribute the high transport distance to the fact that our allocation model underestimates the number of livers that are transported between

OPOs.

However, by imposing a small penalty on the region size, the median distance is reduced substantially. This relationship is demonstrated in Figure 7-3, which plots the tradeoff between V and the two region size metrics - the simulated median distance and the pairwise travel time metric used in the optimization. A small increase in V results in a drastic decrease in median distance, but after some point, increasing V tends to increase the median distance. These results indicate that without the region penalty, the model is minimizing an imperfect measure of organ flow, and therefore sometimes produces regions that are inefficient. By imposing a small penalty on region size, which serves as a proxy for underreported organ shipments, the median distance and time is greatly reduced. However, if V is increased too much, the effect of region size dominates at the expense of reducing within region transport time.

The effect of V can also be seen directly on the region design. Figure 7-4 shows the resulting region design for increasing values of the region penalty for the case when $K = 600$ and the input year is 2015. As expected, regions tend to be large when $V = 0$. But as V is increased, the regions are forced to be smaller.

Figure 7-2: Scatter Plot of MELD Variation and Region Size Penalty

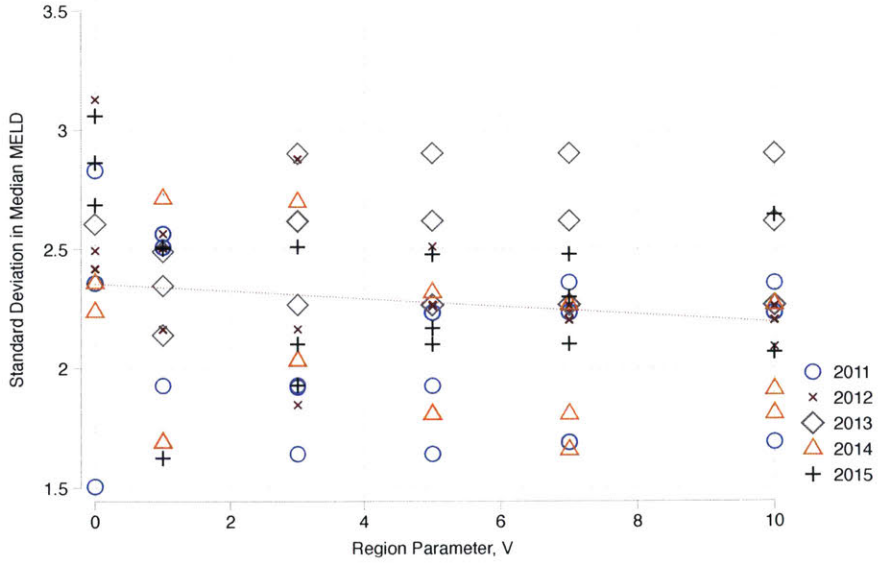

Furthermore, Figure 7-2 shows that the region size penalty has very minimal

systematic impact on the standard deviation of median MELD.

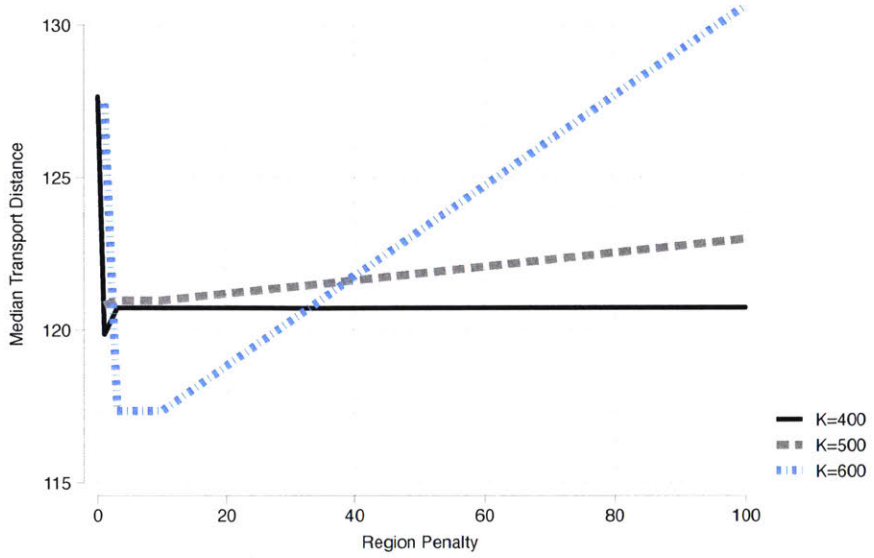

Figure 7-3: Effect of Region Size Penalty (V) on Median Distance

Figure 7-4: Effect of Region Size Penalty (V) on Regions

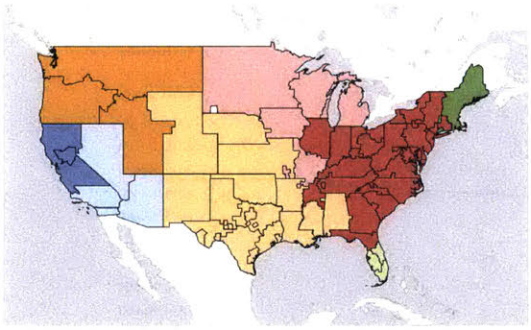

(a) $V = 0$

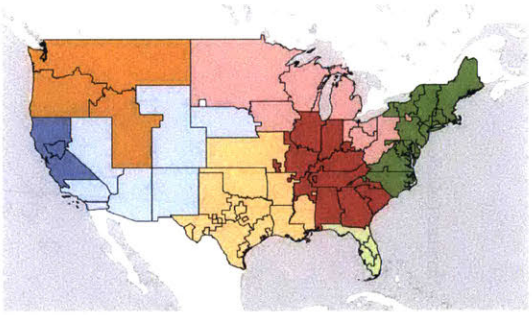

(b) $V = 3$

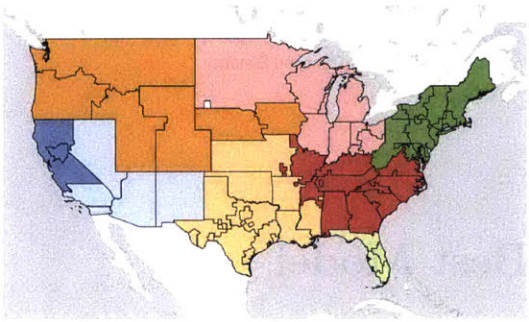

(c) $V = 100$

Relationship between Geographic Variation and Region Size

The relationship between the region size and the geographic variation is much less clear. Figure 7-5 plots the standard deviation in regional median MELD versus the median transport distance for each input year 2011-2015, revealing a line of best fit with a coefficient close to 0. This result, at first glance, may appear to be counterintuitive. Larger regions might be able to better balance supply and demand to create more equal geographical outcomes. However, these results indicate that is not the case in the liver allocation system.

Furthermore, there is no evident pattern between the parameter for allowable geographic variation and the key metrics of the system. In Figure 7-5, the allowable geographic is coded by color. Based on this sample, visual inspection reveals no systematic pattern.

Figure 7-5: Scatter Plot of MELD Variation and Liver Transport Time

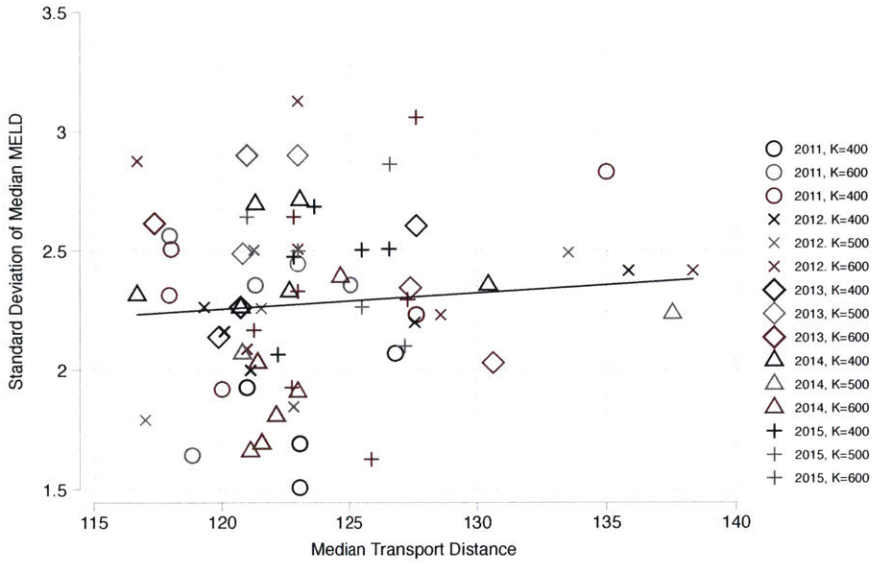

7.5 Selecting Best Model

Table A.6 and Figure 7-5 both demonstrate significant variation in key results depending on the parameters. However, to offer a concrete proposal to alleviate geographic

variation, we need to choose one model. There are several configurations of model parameters that result in reduced geographic variation and low median transport distance.

In addition to the geographic variation and distance metrics, we also consider the configuration's robustness to different years of data, as well as how well the model aligns with our intuition and understanding of the model. Based on those criteria, we select the regions produced by the model with $K = 400$ and $V = 1$ for year 2011. This region configuration has a standard deviation of median MELD of 1.59 and a median distance of 120.9 in the simulation.

We note that other parameter configurations result in lower geographic variation. When $V = 0$ and $K = 400$, the standard deviation of median MELD is 1.51. However, this model results in slightly higher median distance (1.23) Furthermore, we have noted in this chapter that the optimization without a penalty on region size often produces regions with unacceptably high median distances. Therefore, based on our understanding of the model, these results may be an anomaly.

7.6 Sensitivity Analysis

Next, we consider how robust our model is to the varying input years of data. Table 7.1 reports the results for each parameter setting averaged over the 5 years of input. The selected model used in the redistricting proposal in Chapter 3 is noted with asterisks. For most cases, the parameter settings are fairly robust to the year of input data. For instance, for the model with $V = 1$ and $K = 500$, the resulting geographic variation ranges between 1.5 and 2.5.

However, we note that the results are most sensitive to the input data when there is no region penalty. When $V = 0$, the model produced both the lowest geographical variation (1.51) and the highest (3.13) for different years of input data and values of K. The average values of geographical variation are also the highest when $V = 0$, as shown in Table 7.1. Therefore, even though the model with no region penalty produced favorable results in a few cases, these results may be outliers.

		Average of 2011-2015		
K	V	Standard Deviation of Median MELD	Median Distance	Median Time
400	0	2.31	128.12	1.70
	1*	2.29*	122.11*	1.68*
	3	2.31	121.94	1.68
	5	2.25	120.09	1.68
	7	2.18	122.98	1.69
	10	2.10	122.85	1.69
	100	2.30	125.00	1.69
500	0	2.57	128.41	1.70
	1	2.35	120.90	1.68
	3	2.10	122.24	1.69
	5	2.14	122.13	1.69
	7	2.28	122.62	1.68
	10	2.39	121.38	1.68
	100	2.26	123.10	1.68
600	0	3.01	128.54	1.70
	1	2.18	122.32	1.69
	3	2.27	119.63	1.68
	5	2.27	122.26	1.68
	7	2.21	124.40	1.69
	10	2.30	122.35	1.69
	100	2.34	121.85	1.68

Table 7.1: Summary of Results Averaged over Input Years 2011-2015

7.7 Comparison with Baseline

In Chapter 3, we compare the best model with the current 11 region configuration and 2016 OPTN redistricting proposal, and show that our proposal reduces geographic variation with minimal impact on efficiency.

In this section, we compare our approach against a baseline approach which minimizes the sum of absolute differences in rates of supply and demand across regions. The full results for the baseline approach are shown in Table 6.2, and the average over the 5 years is shown in Table 7.2.

Our model consistently produces comparable or superior results than the baseline. Compared to the baseline with a 3 hour travel time constraint, our model consistently results in lower geographic variation and lower median transport time. Compared to the baseline with a 4 hour travel time constraint, the geographic variation is slightly

Table 7.2: Baseline Results: Average of Input Years 2011-2015

Metric	3 Hour Travel Time Max	4 Hour Travel Time Max
S.D. of Median MELD	2.62	2.158
Median Transport Distance (Miles)	1.69	1.69
Median Transport Time (Hours)	127.91	128.82

higher, but our model results in lower transport distance. However, the results for the baseline model are slightly more consistent across input years, suggesting that the baseline model may be more robust.

THIS PAGE INTENTIONALLY LEFT BLANK

Chapter 8

Limitations and Extensions

In this section, we describe the limitations of our current approach and ways to extend the methodology.

8.1 Limitations

8.1.1 Simulation

The validated simulation approach allows us to evaluate many aspects of an allocation policy. However, due to limits on LSAM, results were only simulated for one year. A longer period of simulation would have resulted in a better understanding of the performance of a given allocation rule. In addition, a longer simulation period could assist in selecting model parameters, especially in Model 2. By reserving a subset of the simulation period, the model parameters could be chosen out of sample.

Furthermore, due to time constraints, we were limited to simulating each parameter configuration just once in Model 2. However, to reduce the variance in the simulation results, it would have been preferable to run the simulation for multiple resampled input files.

Lastly, we note limitations of this simulation approach in general. LSAM uses logistic regression to model the acceptance decision, which is estimated based on historical data. Therefore, the simulator does not attempt to model how changes

in allocation rules will affect the candidates' acceptance decision. Therefore, when considering a change in allocation, policy makers also need to consider how agents (donors and candidates) will change their behavior. Currently, this behavior response is beyond the state of the art in allocation modeling.

8.1.2 Computational Limits

Redesigning liver allocation regions is a challenging task, and computational considerations played a key role in this thesis. To overcome computational hurdles, we used an initial region heuristic and aggregated state space. While we argue that these modeling choices do not significantly affect the results, computational considerations did constrain other modeling choices as well. In the absence of computational limits, the two models presented here could be merged into a single model, instead of being solved as complementary problems.

Some previous attempts to redesign liver allocation regions used a very simplified model that abstracts away from many key processes of the allocation system [14]. Others used advanced optimization approaches, together with heuristics, to solve liver redesign optimization systems that modeled key elements of the allocation system. Specifically, branch-and-price, together with a Ryan-Foster branching rule, were shown to be particularly effective for this problem [17]. Although not considered in this thesis, branch-and-price could overcome some of the computational problems so that the model could incorporate other modeling choices.

8.2 Extensions

Both models presented in this thesis contain key processes of the allocation system, such as the waitlist dynamics and allocation rule. As a result, the models are very flexible and allow for the inclusion of policy constraints and alternative modeling choices. In this section, we discuss four extensions of our framework.

8.2.1 Modeling: Acceptance Decision

In the fluid approximation and waterfilling approach, livers were allocated to the highest MELD within each region, and all livers were accepted. In reality, that is not always the case. Candidates reject livers based on a multitude of factors, but the most prominent are high transport distance and quality of the liver (e.g. donor was in poor health). Because we were assuming that all livers were accepted, we had to constrain the degree to which livers were transported long distances. In Model 1, we used constraints on the geographical size of the region, and in Model 2, we minimized the total transport time with a region size penalty. However, if our model incorporated the acceptance decision, the reliance on these geographic measures would not be as necessary, since the acceptance decision would rely on the distance.

Furthermore, the region size used in the objective function of Model 2 served to offset the underestimate of livers being shipped between geographic areas. With an accurate model of liver acceptance, we would see more realistic flows between OPOs. Therefore, incorporating acceptance decision into the model might obviate the need for the region penalty, which primarily served to correct for the underestimation of organ flows. However, incorporating the acceptance decision in an optimization formulation of region design is difficult. Stahl et al. make the assumption that the acceptance decision is only affected by travel time. In reality, the acceptance decision is much more complicated. Therefore, it is not clear that including a greatly simplified model of acceptance would produce better results evaluated on a validated simulation approach, such as LSAM.

8.2.2 Modeling: Financial Cost

One key contribution of the models presented in this thesis is the modeling of flows of livers between geographic areas. Not only does increased transport time reduce the quality of the liver, but it also increases costs. Therefore, minimizing the overall transport distance generally improves the system in more than one way. However, the allocation system also has costs associated with pre- and post-transplant care. Gentry

et al. provided an estimate of the costs of transportation and care [12]. They estimate that under the Share 34 rule, transportation costs constitute $270 million of the $8003 million in total transplantation costs. By including the costs of transportation and care in the optimization model, we could estimate frontier curves that reflect all the different allocation systems are possible for a given system cost.

8.2.3 Modeling: Geographic Variation

This thesis uses two metrics for geographic variation: the variation in median MELD across regions and the absolute sum of differences in rate of supply and demand. Although the variation in median MELD is a key metric used by policy makers to measure geographic variation, it doesn't capture the distribution in MELD at transplant. However, the median MELD formulation presented in Chapter 6 can be extended to model an arbitrary distribution percentile. Therefore, the geographic variation could be captured by a combination of the variation in the median and other key percentiles. By using a more complete metric for geographic variation in the optimization, it might be possible to produce even more equitable region configurations.

8.2.4 Modeling: Impact on Individual OPOs

Liver transplantation is a highly profitable and prestigious business. As a result, there is intense competition over access to donor livers [25]. Mathematical optimization has helped cut through the political landscape, as evidenced by Gentry's work in garnering support for the 2016 OPTN proposal [14]. However, since any redistricting proposal will necessarily have winners and losers, there will always be at least some OPOs that oppose a plan.

Therefore, to make the mathematical optimization approach to redistricting more palatable to stakeholders, one could impose constraints in the formulation that prevent any OPO from losing a significant amount of transplantations. While this might restrict the degree to which geographic variation could be reduced, it also might increase the likelihood of actually implementing a proposal by eliminating any strong

opponents to the plan.

THIS PAGE INTENTIONALLY LEFT BLANK

Chapter 9

Conclusion

In this thesis, we present a new approach to optimizing liver allocation regions to reduce geographic variation. We propose a fluid model to approximate the liver waitlist and allocation process. Then, we formulate two optimization models. Model 1 directly minimizes the variation in median MELD, which is a key metric used by policy makers to measure geographic variation. Then, Model 2 minimizes the total liver transport time subject to some allowable level of geographic variation. We show that Model 2 produces superior results compared to a baseline approach that minimizes the absolute difference in rates of supply and demand. Based on this analysis, we propose a redistricting proposal that reduces geographic variation with very minimal impact on efficiency. Last, we discuss how our flexible modeling approach can be extended to create additional useful models.

THIS PAGE INTENTIONALLY LEFT BLANK

Appendix A

Tables and Figures

Data Disclaimer

The data reported here have been supplied by the Minneapolis Medical Research Foundation (MMRF) as the contractor for the Scientific Registry of Transplant Recipients (SRTR). The interpretation and reporting of these data are the responsibility of the author(s) and in no way should be seen as an official policy of or interpretation by the SRTR or the U.S. Government

Table A.1: Waitlist Candidate Arrivals by DSA: 2015

			MELD Percentile				
Center	DSA ID	Arrivals	10	25	50	75	90
Birmingham, AL	5	149	9	12	17	25	35
Little Rock, AR	10	59	9	13	18	23	35
Phoenix, AZ	19	201	8	11	16	26	36
San Ramon, CA	34	607	7	10	15	22	32
Los Angeles, CA	52	746	8	12	18	31	39
San Diego, CA	61	137	7	9	15	23	33
Denver, CO	88	241	7	10	14	19	29
Annandale, VA	106	110	8	11	14	22	31
Winter Park, FL	115	70	8	12	19	27	37
Miami, FL	124	243	8	12	17	24	34
Gainesville, FL	134	263	9	11	17	24	38
Tampa, FL	138	96	7	12	18	23	32
Norcross, GA	143	378	9	12	17	25	34
Honolulu, HI	157	31	7	10	14	19	28
North Liberty, IA	169	29	9	15	17	25	35
Itasca, IL	176	356	9	12	17	26	34
Indianapolis, IN	200	182	9	12	16	22	30
Louisville, KY	207	145	9	12	17	22	32
Metairie, LA	222	347	8	12	17	24	30
Waltham, MA	302	513	7	10	14	20	30
Baltimore, MD	309	447	7	10	14	23	35
Ann Arbor, MI	330	272	9	11	15	21	29
Minneapolis, MN	346	285	8	11	15	23	33
St Louis, MO	360	172	8	11	16	22	29
Flowood, MS	369	35	9	13	17	30	40
Westwood, KS	374	139	9	11	16	22	27
Charlotte, NC	378	94	9	13	18	25	38
Greenville, NC	390	129	8	12	17	22	30
Omaha, NE	399	135	7	12	16	24	32
New Providence, NJ	411	76	8	11	18	26	36
Rochester, NY	440	57	7	10	21	33	39
New York, NY	450	646	7	10	14	21	34
Cleveland, OH	470	234	7	11	16	23	33
Columbus, OH	472	53	9	13	19	26	37
Cincinnati, OH	480	151	8	11	14	21	30
Oklahoma City, OK	494	97	8	10	14	20	31
Portland, OR	505	103	8	10	15	21	31
Philadelphia, PA	516	537	8	11	16	23	34
Pittsburgh, PA	530	222	8	11	16	23	38
Guaynabo, PR	589	60	8	12	17	23	27
Charleston, SC	596	81	8	14	20	24	33
Nashville, TN	604	182	9	14	18	24	30
Cordova, TN	612	163	9	14	18	24	36
Houston, TX	637	620	8	11	17	27	35
San Antonio, TX	660	271	8	11	17	24	33
Dallas, TX	661	295	8	11	16	27	33
Salt Lake City, UT	692	152	8	12	16	22	33
Virginia Beach, VA	706	142	9	12	17	24	33
Bellevue, WA	730	206	8	12	17	26	36
Madison, WI	747	165	8	13	18	28	37
Bloomfield, CT	766	43	11	13	19	25	36
Milwaukee, WI	832	141	7	10	16	26	35

[1] Excludes 8 DSAs that do not have a transplant center

[2] Includes all adults

Table A.2: Allocation Method for Adult Donors

Order	Candidates within:	And are:
1	OPO's region	Adult or pediatric status 1A
2	OPO's region	Pediatric Status 1B
3	OPO's DSA	MELD/PELD 40
4	OPO's region	MELD/PELD 40
5	OPO's DSA	MELD/PELD 39
6	OPO's region	MELD/PELD 39
7	OPO's DSA	MELD/PELD 38
8	OPO's region	MELD/PELD 38
9	OPO's DSA	MELD/PELD 37
10	OPO's region	MELD/PELD 37
11	OPO's DSA	MELD/PELD 36
12	OPO's region	MELD/PELD 36
13	OPO's DSA	MELD/PELD 35
14	OPO's region	MELD/PELD 35
15	OPO's DSA	MELD/PELD at least 15
16	OPO's region	MELD/PELD at least 15
17	OPO's Nation	Adult or pediatric status 1A
18	OPO's Nation	Pediatric Status 1B
19	OPO's Nation	MELD/PELD at least 15
20	OPO's DSA	MELD/PELD less than 15
21	OPO's region	MELD/PELD less than 15
22	OPO's nation	MELD/PELD less than 15

The chart above shows the allocation for candidates that have identical blood type as the donor. If there is no candidate with identical blood type, the allocation begins from order 1 with candidates that have compatible, but not identical blood type.

Table A.3: 2016 Proposed Allocation Rule for Adult Donors

Order	Candidates within:	And are:
1	OPO's region	Adult or pediatric status 1A
2	OPO's region	Pediatric Status 1B
3	OPO's region	MELD/PELD $\geq$ 29
4	OPO's DSA	MELD/PELD $\geq$ 15
5	OPO's region	MELD/PELD $\geq$ 15
6	Nation	Adult or pediatric status 1A
7	Nation	Pediatric Status 1B
8	Nation	MELD/PELD $\geq$ 15
9	OPO's DSA	MELD/PELD $\geq$ 15
10	OPO's region	MELD/PELD $\geq$ 15
11	Nation	MELD/PELD $\leq$ 15

The chart above shows the allocation for candidates that have identical blood type as the donor. If there is no candidate with identical blood type, the allocation begins from order 1 with candidates that have compatible, but not identical blood type.

Table A.4: Estimated Weekly Transition Probabilities

MELD	6	7	8	9	10	11	12	13	14	15	16	17	18	19	20	21	22	23	24	25	26	27	28	29	30	31	32	33	34	35	36	37	38	39	40	Death
6	92.2	0.4	0.2	0.2	0.4	0.5	0.6	0.7	0.7	0.5	0.4	0.3	0.3	0.2	0.2	0.3	0.4	0.2	0.1	0.1	0.1	0.1	0.0	0.0	0.0	0.0	0.0	0.0	0.0	0.0	0.0	0.0	0.0	0.0	0.0	0.7
7	0.9	96.9	0.6	0.3	0.2	0.1	0.0	0.0	0.0	0.0	0.0	0.0	0.0	0.0	0.0	0.0	0.4	0.0	0.0	0.1	0.0	0.0	0.0	0.0	0.0	0.0	0.0	0.0	0.0	0.0	0.0	0.0	0.0	0.0	0.0	0.2
8	0.6	0.5	96.5	0.6	0.4	0.2	0.2	0.1	0.1	0.0	0.0	0.0	0.0	0.0	0.0	0.0	0.3	0.0	0.0	0.0	0.0	0.0	0.0	0.0	0.0	0.0	0.0	0.0	0.0	0.0	0.0	0.0	0.0	0.0	0.0	0.2
9	0.5	0.2	0.4	96.2	0.8	0.5	0.3	0.2	0.1	0.1	0.0	0.0	0.0	0.0	0.0	0.0	0.2	0.0	0.0	0.0	0.0	0.0	0.0	0.0	0.0	0.0	0.0	0.0	0.0	0.0	0.0	0.0	0.0	0.0	0.0	0.3
10	0.4	0.1	0.2	0.4	96.4	0.8	0.5	0.3	0.2	0.1	0.1	0.0	0.0	0.0	0.0	0.0	0.2	0.0	0.0	0.0	0.0	0.0	0.0	0.0	0.0	0.0	0.0	0.0	0.0	0.0	0.0	0.0	0.0	0.0	0.0	0.2
11	0.8	0.1	0.3	0.8	1.9	92.2	1.5	0.9	0.5	0.2	0.1	0.1	0.1	0.0	0.0	0.0	0.3	0.0	0.0	0.0	0.0	0.0	0.0	0.0	0.0	0.0	0.0	0.0	0.0	0.0	0.0	0.0	0.0	0.0	0.0	0.2
12	1.4	0.0	0.1	0.3	0.9	1.1	92.2	1.4	0.9	0.4	0.2	0.1	0.1	0.0	0.1	0.0	0.3	0.0	0.0	0.0	0.0	0.0	0.0	0.0	0.0	0.0	0.0	0.0	0.0	0.0	0.0	0.0	0.0	0.0	0.0	0.2
13	1.6	0.0	0.1	0.2	0.5	0.7	1.2	92.0	1.3	0.8	0.4	0.2	0.2	0.1	0.0	0.0	0.2	0.0	0.0	0.0	0.0	0.0	0.0	0.0	0.0	0.0	0.0	0.0	0.0	0.0	0.0	0.0	0.0	0.0	0.0	0.3
14	1.5	0.0	0.0	0.1	0.2	0.3	0.7	1.2	92.0	1.3	0.9	0.4	0.3	0.2	0.1	0.1	0.3	0.0	0.0	0.0	0.0	0.0	0.0	0.0	0.0	0.0	0.0	0.0	0.0	0.0	0.0	0.0	0.0	0.0	0.0	0.3
15	1.3	0.0	0.0	0.1	0.1	0.1	0.3	0.7	1.1	92.1	1.2	0.8	0.6	0.3	0.1	0.1	0.3	0.1	0.1	0.1	0.0	0.0	0.0	0.0	0.0	0.0	0.0	0.0	0.0	0.0	0.0	0.0	0.0	0.0	0.0	0.4
16	1.3	0.0	0.0	0.0	0.1	0.1	0.2	0.4	0.7	1.1	91.3	1.5	0.9	0.6	0.4	0.2	0.3	0.1	0.1	0.1	0.0	0.0	0.0	0.0	0.0	0.0	0.0	0.0	0.0	0.0	0.0	0.0	0.0	0.0	0.0	0.4
17	1.1	0.0	0.0	0.0	0.0	0.1	0.1	0.3	0.5	0.7	0.9	91.0	1.5	0.9	0.6	0.4	0.5	0.2	0.1	0.1	0.1	0.1	0.0	0.0	0.0	0.0	0.0	0.0	0.0	0.0	0.0	0.0	0.0	0.0	0.0	0.6
18	0.8	0.0	0.0	0.0	0.1	0.0	0.1	0.1	0.2	0.5	0.6	1.0	90.5	1.4	1.3	0.7	0.6	0.3	0.3	0.1	0.1	0.1	0.1	0.0	0.0	0.0	0.0	0.0	0.0	0.0	0.0	0.0	0.0	0.0	0.0	0.7
19	0.5	0.0	0.0	0.0	0.1	0.1	0.2	0.3	0.6	1.0	1.6	2.3	3.2	81.1	2.9	1.7	1.3	0.6	0.4	0.3	0.2	0.1	0.1	0.1	0.1	0.1	0.0	0.0	0.0	0.0	0.0	0.0	0.0	0.0	0.0	0.8
20	1.5	0.0	0.0	0.1	0.1	0.1	0.1	0.2	0.2	0.4	0.7	0.9	1.5	1.5	85.0	2.6	1.8	0.8	0.4	0.3	0.3	0.2	0.1	0.1	0.1	0.1	0.0	0.0	0.0	0.0	0.0	0.0	0.0	0.0	0.0	1.0
21	2.0	0.0	0.0	0.0	0.0	0.0	0.1	0.1	0.2	0.4	0.4	0.7	1.2	1.0	2.4	83.2	3.2	1.5	0.9	0.6	0.3	0.2	0.1	0.1	0.1	0.1	0.1	0.0	0.1	0.0	0.0	0.0	0.0	0.0	0.0	0.9
22	0.4	0.0	0.1	0.0	0.0	0.0	0.0	0.0	0.0	0.0	0.1	0.1	0.2	0.2	0.3	0.5	93.0	0.6	0.4	2.5	0.1	0.1	0.1	0.1	0.1	0.0	0.0	0.0	0.0	0.0	0.0	0.0	0.0	0.0	0.0	0.9
23	1.3	0.0	0.0	0.0	0.0	0.0	0.0	0.1	0.0	0.1	0.2	0.3	0.4	0.4	0.6	1.0	1.8	86.1	2.1	1.2	0.9	0.6	0.4	0.3	0.2	0.1	0.1	0.0	0.0	0.0	0.1	0.1	0.0	0.0	0.1	1.4
24	1.0	0.0	0.0	0.0	0.0	0.0	0.0	0.0	0.1	0.1	0.1	0.3	0.3	0.2	0.3	0.5	1.1	1.4	86.3	1.9	1.4	1.0	0.5	0.4	0.4	0.3	0.1	0.1	0.1	0.1	0.0	0.1	0.1	0.0	0.1	1.6
25	0.2	0.1	0.1	0.0	0.1	0.0	0.0	0.0	0.0	0.0	0.0	0.1	0.1	0.1	0.1	0.2	0.4	0.6	0.8	91.9	0.6	1.2	2.1	0.1	0.1	0.1	0.1	0.0	0.0	0.0	0.0	0.0	0.0	0.0	0.0	0.9
26	1.0	0.0	0.0	0.0	0.0	0.0	0.0	0.0	0.1	0.1	0.1	0.1	0.2	0.3	0.6	0.7	1.5	2.1	3.5	3.8	73.0	4.1	2.1	1.2	0.8	0.5	0.5	0.2	0.3	0.1	0.1	0.1	0.1	0.1	0.4	1.9
27	0.5	0.0	0.1	0.0	0.1	0.0	0.0	0.0	0.0	0.0	0.1	0.0	0.1	0.1	0.2	0.3	0.5	0.6	1.0	1.0	1.8	86.0	1.5	2.6	0.6	0.3	0.2	0.1	0.1	0.1	0.1	0.1	0.1	0.2	1.4
28	0.3	0.0	0.0	0.0	0.0	0.0	0.0	0.0	0.0	0.0	0.0	0.0	0.0	0.1	0.0	0.1	0.2	0.2	0.4	0.3	0.5	0.6	91.6	2.5	0.6	0.3	0.2	0.1	0.1	0.1	0.1	0.0	0.0	0.0	0.1	1.1
29	0.3	0.1	0.0	0.0	0.0	0.0	0.0	0.0	0.0	0.0	0.0	0.0	0.0	0.0	0.0	0.1	0.1	0.2	0.2	0.3	0.4	0.6	0.7	91.1	0.9	2.0	0.3	0.3	0.1	0.2	0.1	0.1	0.1	0.0	0.2	1.5
30	0.5	0.0	0.0	0.0	0.0	0.0	0.0	0.0	0.0	0.0	0.0	0.0	0.0	0.1	0.1	0.1	0.2	0.3	0.3	0.6	0.7	1.1	1.3	87.8	1.2	1.0	0.6	0.3	0.2	0.2	0.2	0.1	0.1	0.6	2.2
31	0.2	0.0	0.0	0.0	0.0	0.0	0.0	0.0	0.0	0.0	0.0	0.0	0.0	0.0	0.0	0.0	0.1	0.2	0.1	0.3	0.2	0.4	0.5	0.7	0.9	90.0	0.8	1.7	0.4	0.2	0.2	0.1	0.2	0.2	0.5	2.0
32	0.2	0.0	0.0	0.1	0.0	0.0	0.0	0.0	0.0	0.1	0.0	0.0	0.0	0.1	0.1	0.2	0.2	0.2	0.2	0.1	0.3	0.3	0.6	0.6	1.1	0.9	86.1	1.2	1.1	0.7	0.6	0.4	0.2	0.3	0.9	3.0
33	0.2	0.0	0.0	0.0	0.1	0.0	0.0	0.0	0.0	0.0	0.0	0.0	0.0	0.0	0.0	0.2	0.1	0.1	0.2	0.3	0.2	0.3	0.7	0.5	0.6	0.8	87.9	1.2	0.8	0.8	0.3	0.4	0.2	1.2	2.9
34	0.2	0.0	0.0	0.0	0.0	0.0	0.0	0.0	0.0	0.0	0.0	0.0	0.0	0.1	0.1	0.2	0.0	0.0	0.1	0.3	0.1	0.2	0.4	0.3	0.5	0.7	1.0	0.8	85.7	1.5	1.1	0.7	0.5	0.5	1.3	3.6
35	0.1	0.0	0.0	0.0	0.0	0.0	0.0	0.0	0.0	0.0	0.0	0.0	0.0	0.0	0.0	0.1	0.0	0.1	0.0	0.1	0.0	0.1	0.2	0.2	0.3	0.2	0.2	0.6	0.6	89.2	1.0	0.8	0.4	0.4	1.6	3.6
36	0.3	0.0	0.0	0.0	0.1	0.0	0.0	0.0	0.0	0.1	0.0	0.0	0.0	0.0	0.1	0.1	0.0	0.0	0.2	0.1	0.0	0.1	0.2	0.3	0.3	0.4	0.5	0.6	0.6	0.7	84.1	1.4	1.2	1.2	3.0	4.0
37	0.1	0.0	0.0	0.0	0.1	0.0	0.0	0.0	0.0	0.0	0.0	0.0	0.0	0.1	0.0	0.1	0.1	0.1	0.1	0.0	0.1	0.0	0.2	0.1	0.2	0.3	0.2	0.2	0.6	0.4	0.5	88.1	1.3	1.1	2.3	4.0
38	0.2	0.0	0.0	0.0	0.0	0.0	0.0	0.0	0.0	0.0	0.0	0.0	0.0	0.0	0.1	0.0	0.0	0.0	0.0	0.0	0.0	0.1	0.0	0.1	0.1	0.2	0.1	0.2	0.3	0.7	0.9	0.4	85.6	1.9	4.4	4.6
39	0.1	0.0	0.0	0.0	0.0	0.0	0.0	0.0	0.0	0.0	0.0	0.0	0.0	0.0	0.0	0.0	0.1	0.0	0.1	0.0	0.0	0.0	0.1	0.0	0.1	0.0	0.1	0.2	0.1	0.2	0.3	0.2	0.9	88.4	4.9	4.5
40	0.2	0.0	0.0	0.0	0.0	0.0	0.0	0.0	0.0	0.0	0.0	0.0	0.0	0.0	0.0	0.0	0.0	0.0	0.0	0.0	0.0	0.0	0.0	0.0	0.0	0.0	0.0	0.1	0.1	0.1	0.1	0.1	0.2	0.2	92.6	6.0
Death	0.0	0.0	0.0	0.0	0.0	0.0	0.0	0.0	0.0	0.0	0.0	0.0	0.0	0.0	0.0	0.0	0.0	0.0	0.0	0.0	0.0	0.0	0.0	0.0	0.0	0.0	0.0	0.0	0.0	0.0	0.0	0.0	0.0	0.0	0.0	100.0

Table A.5: Aggregated MELD Transition Matrix

State	< 15	15-20	21-22	23-24	25-26	27-28	29-30	31-32	33-34	35-36	37-38	39-40	Death
≤ 15	98.2	0.8	0.4	0.1	0.1	0.0	0.0	0.0	0.0	0.0	0.0	0.0	0.3
15-20	2.9	93.8	1.6	0.5	0.2	0.1	0.1	0.1	0.0	0.0	0.0	0.0	0.6
21-22	1.1	1.7	92.2	1.2	2.3	0.2	0.1	0.1	0.1	0.0	0.0	0.0	0.9
23-24	1.5	1.6	2.2	88.0	2.7	1.2	0.6	0.3	0.1	0.1	0.1	0.2	1.5
25-26	0.6	0.4	0.8	1.9	90.4	3.7	0.5	0.2	0.1	0.1	0.1	0.1	1.1
27-28	0.6	0.3	0.5	1.0	1.6	90.5	3.2	0.5	0.3	0.2	0.1	0.2	1.2
29-30	0.5	0.2	0.2	0.4	0.7	1.5	91.0	2.3	0.6	0.3	0.2	0.4	1.7
31-32	0.4	0.1	0.2	0.3	0.5	0.9	1.6	89.4	2.1	0.7	0.4	0.8	2.3
33-34	0.3	0.1	0.3	0.2	0.4	0.5	1.0	1.5	88.0	2.0	0.9	1.6	3.2
35-36	0.3	0.1	0.1	0.2	0.1	0.3	0.6	0.6	1.3	88.2	1.8	2.8	3.8
37-38	0.2	0.1	0.1	0.1	0.1	0.2	0.2	0.4	0.6	1.2	87.9	4.7	4.3
39-40	0.2	0.1	0.0	0.0	0.0	0.0	0.1	0.1	0.2	0.2	0.4	92.9	5.8
Death	0.0	0.0	0.0	0.0	0a.0	0.0	0.0	0.0	0.0	0.0	0.0	0.0	100.0

Table A.6: Full Results for Varying K, V

Parameters		Optimization Results			Simulation Results		
K	Region Size Parameter	Absolute Difference in Regional Supply and Demand	Total Time of Liver Transport	Total Region Size Metric	SD of Median MELD	Median Travel Time	Median Distance
400	0	388	29.8	1440.2	1.51	123.05	1.69
400	1	368	30.0	1003.5	1.59	120.98	1.68
400	3	368	30.5	1013.1	1.93	120.97	1.68
400	5	368	30.5	1013.1	1.93	120.97	1.68
400	7	368	30.7	1009.2	1.69	123.05	1.69
400	10	394	33.2	975.6	1.69	123.05	1.69
400	100	392	36.0	962.1	2.07	126.83	1.69
500	0	490	29.0	2197.7	2.36	125.06	1.70
500	1	484	29.6	1043.6	2.56	117.94	1.67
500	3	492	30.9	984.3	1.64	118.83	1.68
500	5	496	31.5	969.4	1.64	118.83	1.68
500	7	496	32.0	962.0	2.36	121.30	1.67
500	10	494	33.1	946.7	2.36	121.30	1.67
500	100	494	34.7	931.9	2.45	122.97	1.68
600	0	574	28.2	2217.2	2.83	135.00	1.71
600	1	562	29.6	1020.6	2.51	118.00	1.68
600	3	542	30.3	966.8	1.92	120.00	1.69
600	5	542	30.3	966.8	2.23	127.64	1.69
600	7	598	31.7	943.9	2.23	127.64	1.69
600	10	598	31.7	943.9	2.23	127.64	1.69
600	100	590	35.7	920.6	2.31	117.93	1.68

(a) 2011

Parameters		Optimization Results			Simulation Results		
K	Region Size Parameter	Absolute Difference in Regional Supply and Demand	Total Time of Liver Transport	Total Region Size Metric	SD of Median MELD	Median Travel Time	Median Distance
400	0	396	28.2	1947.6	2.42	135.86	1.70
400	1	386	28.7	1096.9	2.16	120.09	1.68
400	3	386	28.7	1096.9	2.16	120.09	1.68
400	5	396	33.3	966.5	2.26	119.30	1.68
400	7	396	33.0	969.0	2.20	127.58	1.70
400	10	396	33.0	969.0	2.20	127.58	1.70
400	100	394	39.2	932.2	2.00	121.11	1.69
500	0	498	26.3	1726.6	2.49	133.53	1.71
500	1	488	27.8	1083.2	2.50	121.24	1.69
500	3	498	29.1	1022.3	1.85	122.81	1.69
500	5	490	32.8	930.9	2.26	121.53	1.69
500	7	490	32.8	930.9	2.26	121.53	1.69
500	10	490	32.8	930.9	2.26	121.53	1.69
500	100	436	39.2	921.4	1.79	116.99	1.68
600	0	570	25.0	1612.2	3.13	122.97	1.69
600	1	588	28.3	1002.0	2.56	121.81	1.68
600	3	588	28.8	1002.0	2.88	116.66	1.67
600	5	586	30.6	947.5	2.51	122.97	1.69
600	7	598	33.2	904.4	2.23	128.58	1.70
600	10	598	33.2	904.4	2.09	120.97	1.69
600	100	598	34.0	908.9	2.42	138.35	1.71

(b) 2012

Parameters		Optimization Results			Simulation Results		
K	Region Size Parameter	Absolute Difference in Regional Supply and Demand	Total Time of Liver Transport	Total Region Size Metric	SD of Median MELD	Median Travel Time	Median Distance
400	0	394	26.7	2277.3	2.60	127.64	1.70
400	1	394	29.5	962.5	2.14	119.86	1.69
400	3	394	29.9	942.9	2.26	120.73	1.68
400	5	394	29.9	942.9	2.26	120.73	1.68
400	7	394	29.9	942.9	2.26	120.73	1.68
400	10	394	29.9	942.9	2.26	120.73	1.68
400	100	394	29.9	942.9	2.26	120.73	1.68
500	1	498	27.7	1003.2	2.49	120.80	1.68
500	3	492	29.3	922.1	2.90	120.97	1.68
500	5	492	29.3	922.1	2.90	120.97	1.68
500	7	492	29.3	922.1	2.90	120.97	1.68
500	10	492	29.3	922.1	2.90	120.97	1.68
500	100	492	29.8	924.9	2.90	122.97	1.69
600	0	574	25.6	2842.6	2.34	127.42	1.69
600	1	598	26.7	1009.5	2.35	127.42	1.69
600	3	592	28.8	913.4	2.62	117.34	1.68
600	5	592	28.8	913.4	2.62	117.34	1.68
600	7	592	28.8	913.4	2.62	117.34	1.68
600	10	592	28.8	913.4	2.62	117.34	1.68
600	100	534	32.6	908.2	2.03	130.63	1.70

(c) 2013

Parameters		Optimization Results			Simulation Results		
K	Region Size Parameter	Absolute Difference in Regional Supply and Demand	Total Time of Liver Transport	Total Region Size Metric	SD of Median MELD	Median Travel Time	Median Distance
400	0	396	33.0	1636.8	2.36	130.43	1.70
400	1	390	34.6	1017.3	2.71	123.05	1.68
400	3	390	34.8	1001.4	2.70	121.30	1.68
400	5	386	36.6	942.9	2.32	116.66	1.67
400	7	386	36.6	942.9	2.26	120.73	1.68
400	10	386	36.6	942.9	2.26	120.73	1.68
400	100	386	37.0	948.7	2.33	122.64	1.70
500	0	496	32.2	1928.2	2.24	137.55	1.72
500	1	474	33.9	1009.4	1.69	121.55	1.69
500	3	474	34.4	968.0	2.03	121.39	1.69
500	5	420	34.9	954.1	1.81	122.12	1.69
500	7	420	34.9	954.1	1.81	122.12	1.69
500	10	420	34.9	954.1	1.81	122.12	1.69
500	100	456	37.2	943.4	2.07	120.79	1.68
600	0	580	31.6	2576.7	1.69	136.55	1.69
600	1	474	33.9	1009.4	1.69	121.55	1.69
600	3	474	34.4	968.0	2.03	121.39	1.69
600	5	420	34.9	954.1	1.81	122.12	1.69
600	7	420	34.9	954.1	1.66	121.11	1.69
600	10	564	35.0	952.9	1.91	122.97	1.70
600	100	572	41.8	924.3	2.39	124.65	1.69

(d) 2014

Parameters		Optimization Results			Simulation Results		
K	Region Size Parameter	Absolute Difference in Regional Supply and Demand	Total Time of Liver Transport	Total Region Size Metric	SD of Median MELD	Median Travel Time	Median Distance
400	0	400	33.2	1504.9	2.69	123.62	1.69
400	1	372	35.0	1001.4	2.51	126.60	1.69
400	3	372	35.0	1001.4	2.51	126.60	1.69
400	5	372	35.0	1001.4	2.47	122.81	1.68
400	7	388	38.2	956.0	2.47	122.81	1.68
400	10	388	38.2	956.0	2.07	122.18	1.68
400	100	386	39.9	956.1	2.50	125.54	1.69
500	0	484	32.5	3608.9	2.86	126.63	1.70
500	1	498	33.6	1047.1	2.50	122.98	1.68
500	3	498	34.6	971.8	2.10	127.19	1.70
500	5	498	34.6	971.8	2.10	127.19	1.70
500	7	498	34.6	971.8	2.10	127.19	1.70
500	10	462	36.4	949.6	2.64	120.97	1.68
500	100	468	38.2	935.2	2.26	125.54	1.69
600	0	574	32.1	1922.8	3.06	127.64	1.70
600	3	594	34.1	964.8	1.93	122.73	1.68
600	5	598	35.1	941.2	2.17	121.24	1.67
600	7	594	35.2	939.6	2.30	127.31	1.69
600	10	598	36.8	921.8	2.64	122.81	1.68
600	100	598	36.8	921.8	2.33	122.97	1.68

(e) 2015

Bibliography

[1] N Adler. *Location Science References.* 2000.

[2] M. Akan, O. Alagoz, B. Ata, F. S. Erenay, and A. Said. A Broader View of Designing the Liver Allocation System. *Operations Research*, 60(4):757–770, 2012.

[3] O. Alagoz. Incorporating Biological Natural History in Simulation Models: Empirical Estimates of the Progression of End-Stage Liver Disease. *Medical Decision Making*, 25(6):620–632, 2005.

[4] Oguzhan Alagoz, Andrew J. Schaefer, and Mark S. Roberts. Optimizing organ allocation and acceptance. *Springer Optimization and Its Applications*, 26:1–24, 2009.

[5] Dimitris Bertsimas and Sarah Stock Patterson. The air traffic flow management problem with enroute capacities. *Operations research*, 46(3):406–422, 1998.

[6] Mark S. Daskin. Service Science: Application Areas. 2010.

[7] Mehmet C. Demirci, Andrew J. Schaefer, H. Edwin Romeijn, and Mark S. Roberts. An exact method for balancing efficiency and equity in the liver allocation hierarchy. *INFORMS Journal on Computing*, 24(2):260–275, 2012.

[8] DHHS. Organ Procurement and Transplantation Network; Final Rule (42 CFR Part 121). *Federal Register*, 63(63):16296–16338, 1998.

[9] Saleh Elwir and John Lake. Current status of liver allocation in the United States. *Gastroenterology and Hepatology*, 12(3):166–170, 2016.

[10] Richard B. Freeman, Russell H. Wiesner, Ann Harper, Sue V. McDiarmid, Jack Lake, Erick Edwards, Robert Merion, Robert Wolfe, Jeremiah Turcotte, and Lewis Teperman. The new liver allocation system: Moving toward evidence-based transplantation policy. *Liver Transplantation*, 8(9):851–858, 2002.

[11] S. E. Gentry. Impact of Broader Sharing on the Transport Time for Deceased Donor Livers. *Liver Transplantation*, 20(10):1237–1243, 2014.

[12] S. E. Gentry, E. K H Chow, N. Dzebisashvili, M. A. Schnitzler, K. L. Lentine, C. E. Wickliffe, E. Shteyn, J. Pyke, A. Israni, B. Kasiske, D. L. Segev, and David A. Axelrod. The Impact of Redistricting Proposals on Health Care Expenditures for Liver Transplant Candidates and Recipients. *American Journal of Transplantation*, 16(2):583–593, 2016.

[13] S. E. Gentry, A. B. Massie, S. W. Cheek, K. L. Lentine, E. H. Chow, C. E. Wickliffe, N. Dzebashvili, P. R. Salvalaggio, M. A. Schnitzler, D. A. Axelrod, and D. L. Segev. Addressing geographic disparities in liver transplantation through redistricting. *American Journal of Transplantation*, 13(8):2052–2058, 2013.

[14] Sommer Gentry, Eric Chow, Allan Massie, Dorry Segev, Allan Massie, and Dorry Segev. Gerrymandering for Justice :. (October 2016), 2015.

[15] Julie Heimbach. OPTN / UNOS Liver and Intestinal Organ Transplantation Committee Meeting Summary Chicago , Illinois Ryutaro Hirose , MD , Chair. Technical Report June 2009, 2016.

[16] P. S. Kamath, R. H. Wiesner, M. Malinchoc, W. Kremers, T. M. Therneau, C. L. Kosberg, G. D'Amico, E. R. Dickson, and W. R. Kim. A model to predict survival in patients with end-stage liver disease. *Hepatology*, 33(2):464–470, 2001.

[17] N. Kong, a. J. Schaefer, B. Hunsaker, and M. S. Roberts. Maximizing the Efficiency of the U.S. Liver Allocation System Through Region Design. *Management Science*, 56(12):2111–2122, 2010.

[18] OPTN/UNOS. Redesigning Liver Distribution to Reduce Variation in Access to Liver Transplantation. Technical report, 2014.

[19] OPTN/UNOS. Redesigning Liver Distribution: Public Comment Proposal. Technical report, 2016.

[20] E. A. Pomfret, J. P. Fryer, C. S. Sima, J. R. Lake, and R. M. Merion. Liver and intestine transplantation in the United States, 1996-2005. *American Journal of Transplantation*, 7(SUPPL. 1):1376–1389, 2007.

[21] Mettu Srinivas Reddy, Joy Varghese, Jayanthi Venkataraman, and Mohamed Rela. Matching donor to recipient in liver transplantation: Relevance in clinical practice. *World Journal of Hepatology*, 5(11):603–611, 2013.

[22] Takeshi Shirabe. Districting modeling with exact contiguity constraints. *Environment and Planning B: Planning and Design*, 36(6):1053–1066, 2009.

[23] Lena Sibulesky, Meng Li, Ryan N. Hansen, Andre A S Dick, Martin I. Montenovo, Stephen C. Rayhill, Ramasamy Bakthavatsalam, and Jorge D. Reyes. Impact of cold ischemia time on outcomes of liver transplantation: A single center experience. *Annals of Transplantation*, 21:145–151, 2016.

[24] J. E. Stahl, N. Kong, S. M. Shechter, A. J. Schaefer, and M. S. Roberts. A Methodological Framework for Optimally Reorganizing Liver Transplant Regions. *Medical Decision Making*, 25(1):35–46, 2005.

[25] Sheryl Gay Stolberg. Iowa turf war over transplants mirrors feuds across the nation. *The New York Times*, pages A1–A18, 1999.

[26] Russell Wiesner, Erick Edwards, Richard Freeman, Ann Harper, Ray Kim, Patrick Kamath, Walter Kremers, John Lake, Todd Howard, Robert M. Merion, Robert A. Wolfe, Ruud Krom, Paul M. Colombani, Paige C. Cottingham, Stephen P. Dunn, John J. Fung, Douglas W. Hanto, Sue V. McDiarmid, John M. Rabkin, Lewis W. Teperman, Jeremiah G. Turcotte, and Lynn Rothberg Wegman. Model for end-stage liver disease (MELD) and allocation of donor livers. *Gastroenterology*, 124(1):91–96, 2003.

[27] Jiaquan Xu, Kenneth D Kochanek, and Sherry L Murphy. National Vital Statistics Reports Deaths : Final Data for 2011. *Statistics*, 63(3):135, 2015.